Universidade de Lisboa
Faculdade de Medicina de Lisboa

Development of a new cellular model for the visualization and study of GFAP oligomerization in living cells

Ricardo José Letra Vilela Ribeiro

Dr. Federico Herrera
Dra. Ana Sebastião

Dissertação especialmente elaborada para obtenção do grau de mestre em Neurociências

2015

A impressão desta dissertação foi aprovada pelo Conselho Científico da Faculdade de Medicina de Lisboa em reunião de 28 de Outubro de 2014.

Universidade de Lisboa
Faculdade de Medicina de Lisboa

Development of a new cellular model for the visualization and study of GFAP oligomerization in living cells

Ricardo José Letra Vilela Ribeiro

Dr. Federico Herrera
Dra. Ana Sebastião

Dissertação especialmente elaborada para obtenção do grau de mestre em Neurociências

ANICT – Associação Nacional de Investigadores em Ciência e Tecnologia
ITQB – Instituto de Tecnologia Química e Biológica
FCT – Fundação para a Ciência e Tecnologia

2015

Todas as afirmações efectuadas no presente documento são da exclusiva responsabilidade do seu autor, não cabendo qualquer responsabilidade à Faculdade de Medicina de Lisboa pelos conteúdos nele apresentados.

A impressão desta dissertação foi aprovada pelo Conselho Científico da Faculdade de Medicina de Lisboa em reunião de 28 de Outubro de 2014.

Acknowledgements

I would like to mention all the people that made the development of this thesis possible, personally and academically:

To my supervisor Dr. Federico Herrera, for the opportunity to work in his laboratory, for all the patience and all the dedicated time during the whole year, thank you. Also thank you for all the transmission of knowledge and the good advice that allowed me to grow personal and scientifically.

To my co-supervisor Dr. Ana Sebastião for her support throughout this thesis. Thank you for all the time dispended to promptly answer all my questions and for helping me to decide and find something to work that meets my wishes. Also thanks for the continuous preoccupation.

I would like to give special thanks to Dr. Mariana Santa-Marta for all the help during my thesis, giving me different points of view in the time that I faced some difficulties. Also thanks for the scientific discussions and talks.

Thanks to Dr. Isabel Pacheco for all the support in laboratory during the last year.

To all the persons that gave me technical support in microscopy and flow cytometry facilities at IGC.

To my parents, Luisa Letra and José Vilela, my grandmother, Maria Clara, my girlfriend, Bruna Abrunhosa, my friends André Cardoso, Gonçalo Valente, Kumar, Gonçalo Toste and others, thank you for your support and for keeping me motivated and focused during all the year. Thank you for believing in me and for helping me in all the stages of my live.

And last but not least, I would like to thank the anonymous person who made this dream possible, who allowed me to begin this course and gave me all the necessary conditions to do my best work for the past two years. Without him, this thesis would not have been possible.

Ricardo José Letra Vilela Ribeiro boasts an ANICT fellowship for the development of Master's thesis titled “Development of a new cellular model for the visualization and study of GFAP oligomerization in living cells”.

Abstract

Intermediate Filaments are one of the major components of the cell cytoskeleton. They have an important role during stress and tissue damage. In the central nervous system, astrocytes are the most abundant cell type, and GFAP is the main component of astrocytic filaments. GFAP is involved in the reaction of astrocytes to CNS damage and it is associated to several diseases inside and outside the CNS, such as Alexander Disease, Crohn's Disease.

Although GFAP was discovered in 1971, there is still no good model to study its oligomerization in living cells. The main goal of this study is to develop a new cellular model for the visualization and study of GFAP oligomerization in living cells.

Our model is based on bimolecular fluorescence complementation (BiFC) assays, which have been widely used to study protein-protein interactions in living cells. Briefly, GFAP was fused to two non-fluorescent halves of the Venus yellow fluorescent protein. When GFAP dimerizes, the Venus halves should get together and reconstitute the fluorophore. Fluorescence should therefore be proportional to the amount of GFAP dimers/oligomers.

We have tested three different BiFC pairs, but only one produced a fluorescence signal. However, its pattern of intracellular distribution

does not match the normal GFAP fibrillary pattern. Instead, it produces a cytoplasmic signal with a rather heterogeneous distribution. When GFAP interacts with other proteins produces a different pattern specific of each interaction partner, producing aggregates in some cases. This suggests that GFAP behavior is only partially dependent on the tag, and can be modified by the intracellular context.

Further studies with all the possible combinations of venus halves in both N- and C-termini, or within GFAP, are needed to know if a BiFC system for GFAP or other intermediate filaments is actually possible.

Keywords: Intermediate Filaments; GFAP; Oligomerization; Alexander Disease; BiFC system

Resumo

O citoesqueleto desempenha um importante papel na sobrevivência e comportamento celular. É responsável pela organização espacial dos conteúdos celulares, conectando fisicamente e bioquimicamente a célula ao ambiente externo e gerando forças coordenadas que permitem a célula a alterar a sua forma e a mover-se. Os filamentos intermédios são um dos principais componentes do citoesqueleto celular. Estes têm um papel especialmente importante durante o stress e dano dos tecidos.

No sistema nervoso central, os astrócitos são o tipo celular mais abundante. Os astrócitos têm funções importantes tanto na doença como na saúde. As ligações moleculares formadas pelos astrócitos guiam a migração dos axónios em desenvolvimento e alguns neuroblastos durante a formação da matéria branca e cinzenta. Os astrócitos também estão envolvidos na transmissão sinática, na maturação dos oligodendrócitos e na mielinização dos nervos. Em condições patologicas tais como doenças neurodegenerativas, os astrócitos reagem, tornam-se hipertróficos e proliferam para pôr límite ao dano. Se a barreira hematoencefalica é danificada, eles forman uma cicatriz e fecham a ferida, limitando assim a extensão da lessão.

A proteina ácida fibrilar glial (GFAP) é a principal componente dos filamentos astrociticos. A GFAP está envolvida na reação dos astrócitos

ao dano no sistema nervoso central e está associada a várias doenças dentro e fora do sistema nervos central, tais como a doença de Alexander ou a doença de Crohn's. A GFAP é também o principal marcador para a identificação de astrócitos, e o seu promotor é utilizado de uma forma extensiva para a expressão de genes específicos em astrócitos. A GFAP tende a formar filamentos de 10 nm. Em primeiro lugar duas moléculas de GFAP ligam-se uma à outra e formam dímeros, que por sua vez ligam-se a outros dímeros dando origem a protofilamentos. Por último estes protofilamentos tendem a juntar-se e formar então os filamentos maturos. Quando a GFAP é sobreexpresa ou sofre mutações, como acontece em alguns tipos de cancro e na doença de Alexander, a GFAP forma agregados fibrilares patológicos conhecidos como fibras de Rosenthal.

Apesar da GFAP ter sido descoberta em 1971 ainda não há um bom modelo que permita o estudo da sua oligomerização em células vivas. Até agora, todas as tentativas de visualização da oligomerização resultam em padrões difusos e de agregação da GFAP ao contrário do aspeto normal de filamentos intermédios. Com isto, o principal objetivo deste estudo é desenvolver um novo modelo celular para a visualização e estudo da oligomerização da GFAP em células vivas.

O nosso modelo é baseado no sistema de ensaios de fluorescência por complementação bimolecular (BiFC) que tem sido amplamente utilizado para estudar interações entre proteínas em células vivas. Este

sistema tem como base a utilização de duas metades não fluorescentes de uma proteína fluorescente que são acopladas a uma proteína de interesse. Aquando a interação das proteínas de interesse, as metades não fluorescentes vão interagir e reconstituir o fluoróforo. A fluorescência originada permite assim calcular, indiretamente, os níveis de dimerização da proteina de interesse e a localização intracelular dos dímeros. A criação do sistema é feita de uma maneira empírica, havendo uma série de possibilidades tanto no local de corte da proteína fluorescente como na localização destas em relação à proteína fluorescente. Diferentes tamanhos das metades não fluorescentes levam a diferentes níveis de background o ao tratamento prévio das células para potenciar os níveis de fluorescência. O acoplamento à proteína de interesse pode ser na parte N- ou C-terminal, e pode levar um linker entre a metade fluorescente e a proteína de interesse para incrementar a flexibilidade da fusão.

Resumidamente, a GFAP foi ligada a duas metades não fluorescentes da proteína fluorescente amarela Venus. Quando a GFAP dimeriza, as metades da Venus juntam-se e reconstituem o fluoróforo. A fluorescência é proporcional à quantidade de dímeros/oligómeros de GFAP.

Testámos três combinações diferentes dos constructos de BiFC GFAP-Venus. Todas as combinações incluíam o plasmídeo Venus 1 – GFAP emparelhado com três plasmídeos de Venus 2 – GFAP diferentes,

sendo eles GFAP - Venus 2 (amino ácidos 158-238), GFAP – Venus 2 (amino ácidos 210-238) e Venus 2 (amino ácidos 210-238) - GFAP. Apenas o primeiro apresentou fluorescência. Isto não foi devido a diferenças ou deficiências na expressão da GFAP, que foi confirmada por meio de anticorpos específicos e ensaios western blot em todos os cassos. Contudo, em comparação com outros sistemas de BiFC já desenvolvidos, os níveis de fluorescência foram reduzidos. Quando verificamos através de microscopia o comportamento da GFAP, o seu padrão de distribuição intracelular não coincide com o padrão normal de fibrilação. Ao invés, produz um sinal citoplasmático com uma distribuição heterogénea. Fibras de Rosenthal ou outros padrões de agregação não foram observados, no entanto como já foi referido anteriormente o sinal não delineava a rede de filamentos intermédios regular.

Em seguida, de modo a verificar se a GFAP interagia com outras proteínas e também produzia padrões de agregação, transfetou-se células com o plasmídeo GFAP – Venus 1 em combinação com outros plasmídios carregando proteínas relacionadas com neurodegeneração ligadas a Venus 2. Um grupo dessas proteínas está diretamente envolvido em doenças neurodegenerativas, com uma forte tendência para agregação e localizadas principalmente no citosol, que inclui a huntigtina, a proteina tau, a synucleina e a DJ-1. O outro grupo de proteínas é maioritariamente constituído por factores de transcrição (STAT3 e p53) ou os seus

reguladores (mdm2), e usualmente não produz agregados estando localizadas no núcleo e citosol. Quando a GFAP interage com outras proteínas produz um padrão diferente especifico de cada proteína de interação, produzindo agregados em alguns casos. No primeiro grupo produz níveis de fluorescência maiores em comparação com o segundo grupo. Estes resultados sugerem que o comportamento da GFAP é apenas parcialmente dependente do tag e pode ser modificado pelo contexto intracelular.

No presente estudo, não foi possível desenvolver, até à data, um sistema de BiFC que permita a visualização e estudo da GFAP normal e aberrante. No entanto foi possível retirar algumas conclusões. A partição das metades não fluorescentes 1 a 210 e 210 a 238 não é funcional, pelo menos no contexto da proteína GFAP, ou seja, não há sinal de fluorescência. O único par funcional de todos os testados não reproduz a distribuição intracelular esperada para a GFAP apesar de apresentar níveis de fluorescência. Também se verificou que a GFAP pode co-agregar seletivamente com várias proteínas relacionadas com doenças neurodegenerativas.

Mais estudos com todas as possíveis combinações das metades da Venus nos terminais N- e C-, ou dentro da GFAP, são necessários para perceber se um sistema BiFC para a GFAP ou outros filamentos intermédios é realmente possível. Um sistema assim permitiria analizar os

mecanismos moleculares da formação de oligomeros e fibras normais ou aberrantes (Rosenthal fibers) da GFAP. Por causa do importante papel dos astrócitos e da GFAP na reação ao dano no sistema nervoso central e nos plexos nervosos do intestino, o nosso modelo podería contribuir à compreensão e tratamento dum grande número de doenças humanas tais como as doenças de Alzheimer o Parkinson, acidentes cerebro-vasculares, trauma cerebreal o espinal, o a doença de Crohn.

Palavras chave: Filamentos intermédios; GFAP; oligomerização; doença de Alexander; BiFC

General Contents

Index of images

List of abbreviations

A.a. Amino acids

AxD Alexander Disease

BiFC Bimolecular fluorescent complementation

BSA Bovine Serum Albumine

CNS Central Nervous System

pCMV Cytomegalovirus promoter

GFAP Glial Fibrillary Acidic Protein

HSCs Hepatic stellate cells

IFs Intermediate filaments

LB Luria Broth

RT Room Temperature

SCs Schwann cells

TBS Tris-HCl buffer saline

HCV Virus Chronic Hepatitis

1. Introduction

1.1 - The cytoskeleton

The cytoskeleton has an important role in cell survival and behavior. It is responsible for organizing spatially the cell contents, connecting biochemically and physically the cell to the external environment, and generating coordinated forces that enable the cell to change shape and move. These functions are possible because the component polymers and regulatory proteins of the cytoskeleton are in a constant flux and have a dynamic and adaptive structure (Fletcher & Mullins 2010).

The cytoskeleton of most animal cells is composed of three major fiber systems: microfilaments (6 nm in diameter), intermediate filaments (10nm in diameter) and microtubules (24 nm in diameter). Microfilaments are universal scaffolds and force-providing molecules that are used for a wide range of processes that require form and force. Microtubules are involved in maintenance of cell shape, transport, motility, and division. Finally, intermediate filaments allow cells to functionally integrate the corresponding cytoskeletal systems with the physiological requirements of individual tissues and entire organs, and

are especially important under stress conditions (Nishizawa et al. 1991; Gunning et al. 2015; Nogales 2001; Herrmann et al. 2007).

Intermediate filaments

Intermediate filaments (IFs) are divided into six main types according to their tissue-restricted distribution (Figure 1). All of them share the same structural organization, with a central α-helical rod domain flanked by amino- and carboxy-termini of variable sizes. Phosphorylation and dephosphorylation of these flanking regions have a critical role for the maintenance and reconstruction of IFs (Bongcam-Rudloff et al. 1991; Eliasson et al. 1999; Nishizawa et al. 1991).

Type	Protein	Size (Kd)	Site of Expression
I	Acidic keratins	40-60	Epithelial cells
II	Neutral or basic keratins	50-70	Epithelial cells
III	Vimentin	54	Fibroblasts, white blood cells, and other cell types
	Desmin	53	Muscle cells
	Glial Fibrillary Acidic Protein	51	Glial cells
	Peripherin	57	Peripheral neurons
IV	**Neurofilament proteins**		
	NF-L	67	Neurons
	NF-M	150	Neurons
	NF-H	200	Neurons
	α-Interneuxin	66	Neurons
V	Nucleal Lamins	60-75	Nuclear lamina of cell types
VI	Nestin	200	Stem cells of central nervous system

Figure 1 - Classification of intermediate filaments

IFs have an essential role in cells during stress, when a maximal cellular response is required to end with an imminent threat. Knockout of astrocytic intermediate filaments blocks hypertrophy of reactive astrocytes in a mice model of entorhinal cortex lesion (Wilhelmsson et al. 2004). Highly abundant cytoskeletal keratins with the conserved S73-containing phosphoepitope serve as a phosphate "sponge" for stress-activated kinases, and thus protect tissues from injury (Ku & Omary 2006).

1.2 - Glial fibrillary acidic protein (GFAP)

Glial Fibrillary Acidic Protein (GFAP) was described for the first time in 1971 as the major component of astrocytic filaments (Eng et al. 1971). Since then, GFAP has become the prototypical marker for the identification of astrocytes, although not all populations of astrocytes express it (Sofroniew & Vinters 2010). The GFAP promoter is also extensively used to target the expression of specific genes to astrocytes (Brenner et al. 1994).

Astrocytes are the most abundant cell type of the brain, and have important functions in health and disease. The molecular boundaries formed by astrocytes guide the migration of developing axons and certain neuroblasts during development of gray and white matters (Powell & Geller 1999). Astrocytes regulate synaptic transmission by releasing

synaptically active molecules, including purines (adenosine and ATP), GABA, glutamate and D-serine (Halassa et al. 2007; Nedergaard et al. 2003; Perea et al. 2009). Astrocytes are also involved in oligodendrocyte maturation and nerve myelination (Back et al. 2005), and defects in astrocytes could produce white matter degeneration (Sawaishi 2009). Astroglial end-feet are an essential component of the blood-brain barrier that regulates the access of molecules in the blood flow to the nervous tissue (Sofroniew & Vinters 2010). When there is an injury in Central Nervous System (CNS), astrocytes grow in size and become hypertrophic, secreting cytokines that promote neuroinflammation and neuronal survival (Sofroniew & Vinters 2010). If the blood-brain barrier is damaged astrocytes proliferate and form a glial scar. This glial scar is formed by glial cells produced de novo, and not by migration of pre-existing glial cells, as formation of the glial scar does not coincide with an overall reduction of astrocyte number elsewhere in the CNS (Carmen et al. 2007).

GFAP is very important for astroglial function. It contributes to the ability of astrocytes to cope with oxidative stress and other insults. For example, mice lacking GFAP are more sensitive to ischemic stroke (De Pablo et al. 2013). Upregulation of GFAP expression is a hallmark of reactive astrocytes and responsible for their hypertrophy (Hol & Pekny 2015), although this increase can have different intensities in different regions of the CNS and populations of astrocytes (Jany et al. 2013).

While GFAP is best known as an astroglial protein, it is present in other cell types throughout the body. GFAP expression in the liver is correlated with fibrosis progression in the model of post-transplant recurrent virus chronic hepatitis (HCV). GFAP is used as a marker of early activation of hepatic stellate cells (HSCs) in HCV and its expression levels are related with the severity of the disease (Carotti et al. 2007). GFAP was also found in Schwann cells (SCs) in certain demyelinating and axonal neuropathies (Bianchini et al. 1992); in human lymphocytes (Riol et al. 1997); in supporting cells of the enteric nervous system in Hirschsprung's disease (Kato et al. 1990); and in primary precursors of new neurons in the adult mammalian olfactory bulb and in the dentate gyrus in the hippocampus (Seri et al. 2001; Garcia et al. 2004).

Although GFAP is expressed by several cell types, especially in conditions of stress or inflammation, it is not an essential protein. GFAP-null mice show no overt phenotypes in their development, fertility, and gross CNS morphology and behavior (McCall et al. 1996). GFAP-null astrocytes also have a normal morphology and distribution without any detectable deficiency of neuronal development, and produce a normal blood-brain barrier (Gomi et al. 1995). It has been suggested that vimentin and nestin, or other intermediate filaments, compensate GFAP deficits (Triolo et al. 2006). However, mice lacking GFAP are more sensitive to insults, suggesting an important role for GFAP in CNS response to

damage (Nawashiro et al. 1998). Further studies should be carried out to elucidate the role of GFAP in astroglial behavior and function, and its implications for brain physiology and pathology.

GFAP structure and isoforms

The GFAP gene is localized in chromosome 17, band q21 and it contains nine exons. The final protein has 432 Amino acids (A.a) and a molecular weight of 50 KDa (Isaacs et al. 1998; Bongcam-Rudloff et al. 1991; Kumanishi et al. 1992).

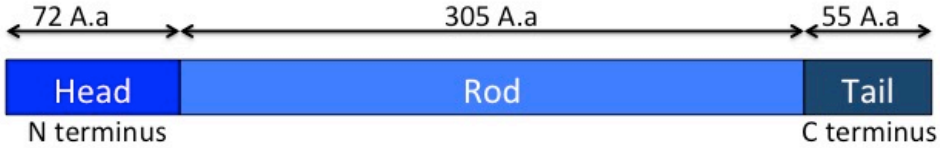

Figure 2 - Schematic representation of GFAP - GFAP have 432 Amino acids (A.a) and is divided in three domains, the Head (1-72 Aa), the Rod (73-377 Aa) and the Tail (378-432 Aa).

GFAP has the structural organization typical of an IF, with a head with 72 amino acids, a Rod domain with 305 amino acids and a non alpha-helical tail with 55 amino acids that shares some phosphorylatable residues with vimentin, suggesting an important role of these sites for IF protein function (Reeves et al. 1989; Geisler & Weber 1983).

Alternative splicing originates 7 different GFAP isoforms in humans, GFAP α, GFAP γ, GFAP Δ164, GFAP Δ135, GFAP Δexon6, GFAP δ/ε and GFAP κ, being GFAP α the most abundant and the first

identified (Reeves et al. 1989; Zelenika et al. 1995; Nielsen et al. 2002; Roelofs et al. 2005; Blechingberg et al. 2007; Hol et al. 2003).

Oligomerization

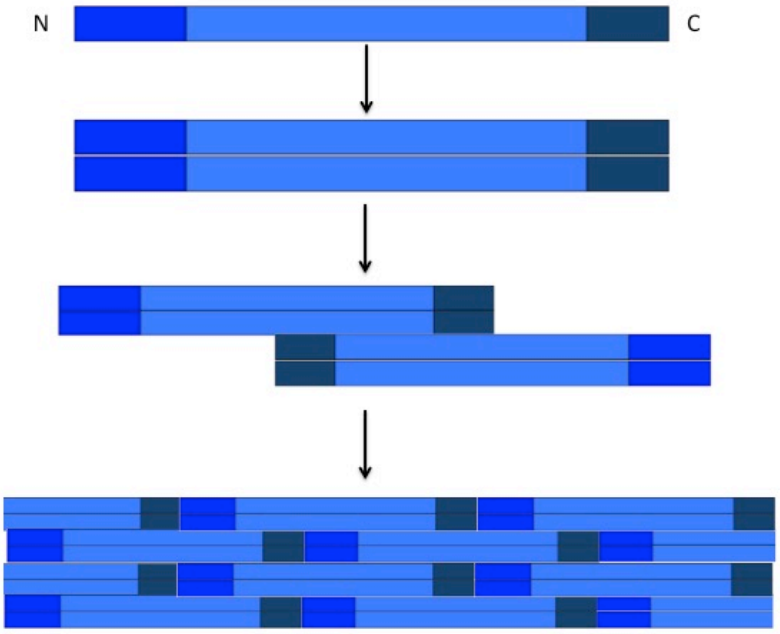

Figure 3 - GFAP oligomerizes to form filaments - Under physiological conditions, two GFAP molecules gather to form a parallel dimer structure, and dimers subsequently assemble to form an anti-parallel tetrameric protofilament. Protofilaments then assemble to form the final 10 nm filament structure.

GFAP tends to form 10 nm filaments in vitro (Rueger et al. 1979). Two GFAP molecules bind to each other and form a parallel alfa-helical coiled-coil dimer structure. Then, dimers bind to other dimers and form an antiparallel tetrameric protofilament. This protofilament with an anti-parallel arrangement characterizes the non-polarized structure of GFAP.

Finally, the protofilaments assemble and constitute the final 10 nm filament (Inagaki et al. 1994).

This process is controlled by diverse factors, such as ionic strength, MgCl2 and CaCl2 concentrations, protein chaperones or phosphorylation of specific residues (Inagaki et al. 1990). Phosphorylation of soluble GFAP leads to a nearly complete inhibition of filament formation (Inagaki et al. 1990).

1.2- Alexander Disease

Alexander Disease (AxD) was described by W. Stewart Alexander in 1947, as a case of mental retardation in an infant with hydrocephalus. In the histological examinations, large numbers of fuchsinophil bodies were found in white matter and beneath both the ependyma and the pia, but sparing the cortex. They showed a characteristic perivascular predominance and these bodies were thought to be a product of fiber degeneration and cell bodies of the fibrillary neuroglia (Alexander 1947). However, the link between GFAP mutations and AxD was not discovered until 2001 (Brenner et al. 2001).

AxD is rare disease with an incidence of approximately 1:1,27 million, although experts think that it is frequently misdiagnosed and that the incidence could be higher (Quinlan et al. 2007). Ninety five per cent of

the cases show mutations in the GFAP gene, while the causes of the other 5% are not known (Yoshida et al. 2011). AxD can be divided in three types: Infantile (0-2 years), Juvenile (2-12 years) and Adult (more than 12 years). Lifespan is related with the age of onset, early onset having a survival rate of 14 years and late onset having a survival rate of 25 years (Russo et al. 1976; Prust et al. 2011).

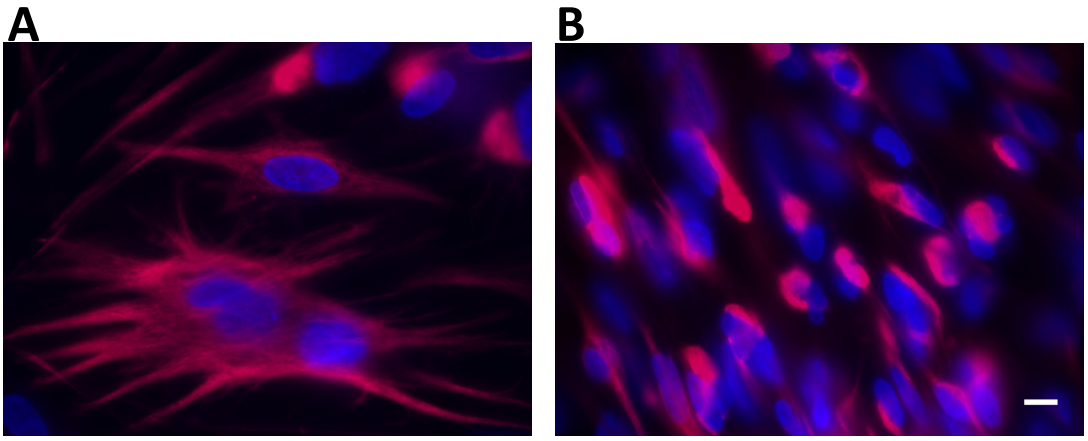

Figure 4 - Mutant GFAP aggregates and forms Rosenthal fibers in glial cells which is one of the histopathological hallmarks of the disease - For this reason AxD belongs to the superfamily of protein misfolding disorders, as Parkinson Alzheimer or Huntington diseases. A) Glial cells showing a normal distribution o GFAP. B) Glial cells with Rosenthal Fibers. GFAP is stained in red and nuclei ar counterstained with DAPI (blue) Scale: 50µm

Nowadays, there are a lot of studies involving GFAP to understand how an alteration in the protein or in the normal behavior of GFAP leads to the development of Alexander Disease. In 2011 it was shown that, altering GFAP protein levels can be one possible factor that leads to AxD (Chen et al. 2011). This aberrant expression leads to a formation of complex structures called Rosenthal Fibers in astrocytes, in a way that can

be lethal, and it is a primary pathological event (Messing et al. 1998; Tang et al. 2006).

Five C-terminal domain mutations in GFAP are linked to AxD because they affect the in vitro assembly and network formation of GFAP in transiently transfected tissue culture cells. The effects seen on GFAP assembly strongly suggest that the mutations affect the formation and subsequent annealing of the unite length filament (Chen et al. 2011). Other studies have tried to understand how many mutations can occur and where, and they say that there are 16 glutamic acid mutations and 31 arginine mutations in GFAP (Szeverenyi et al. 2008).

GFAP aggregation leads to sequestration of small heat shock proteins (sHSPs), activation of p38 stress kinase and a greater decline in cell viability (Chen et al. 2011). Rosenthal fibers could also impair proteasome activity and increase the susceptibility to stress (Bachetti et al. 2012). One possibility for this impairment is that accumulated GFAP saturates the capacity of free cytosolic ubiquitin or molecular chaperones required for UPS function, but another possibility is that GFAP could interact with the proteasome and retain it in inclusions (Tang et al. 2006).

Because AxD is a rare disease mostly affecting newborns, research has been made mostly at an academic level, and the mechanisms and possible disease-modifying pathways remain mostly unknown.

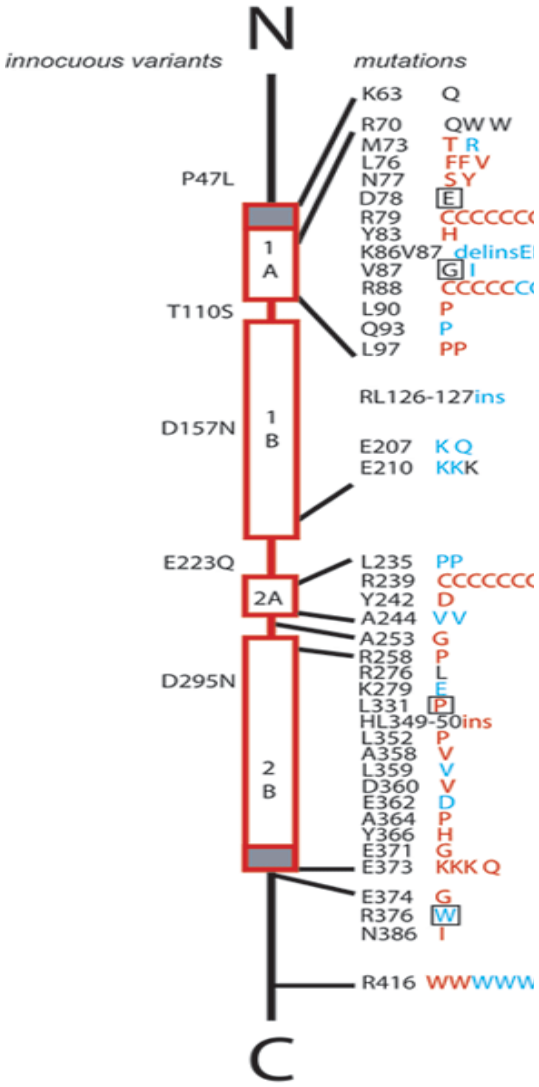

Figure 5 - Diagram of GFAP mutations in relation to protein domains and clinical classification – This diagram is reproduced with the permission of Dr. Albee Messing from the University of Wisconsin: http://www.waisman.wisc.edu/alexander-disease/diagram.html

1.3- BiFC

Bimolecular fluorescent complementation (BiFC) assay is a relatively recent method to study protein-protein interactions in living

cells. Briefly, the interaction partners are fused to two non-fluorescent fragments of a fluorescent reporter. When the proteins of interest interact, the fragments come together, reconstitute the native structure of the fluorophore and emit fluorescence (Morell et al. 2008).

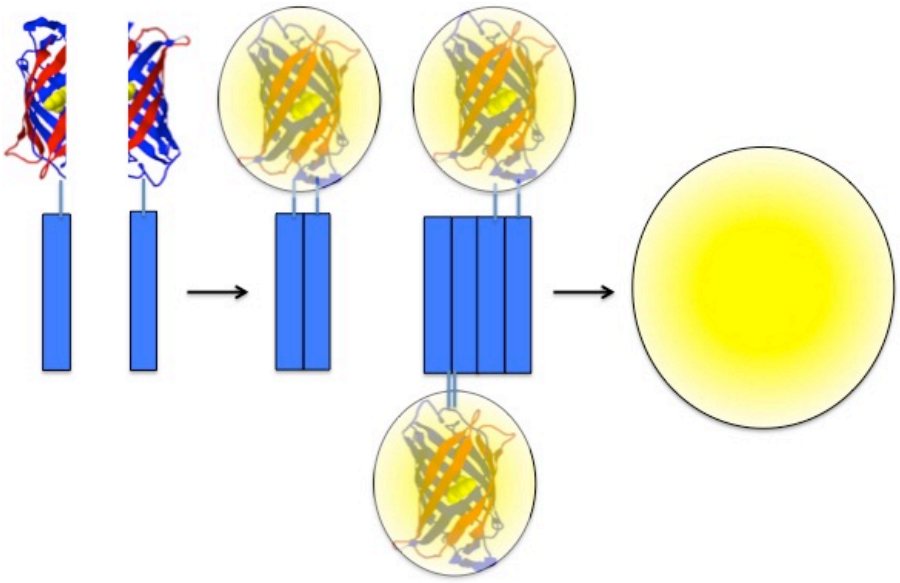

Figure 6 - Bimolecular fluorescence complementation (BiFC) assays for the visualization of protein-protein interactions in living cells - The proteins of interest are fused to two non-fluorescent halves of a reporter protein. We use Venus, a third-generation yellow fluorescent protein that has been optimized for this type of assay. When the proteins of interest dimerize/oligomerize, the two Venus halves get together and reconstitute the functional fluorophore. Fluorescence can be measured by conventional methods, such as flow cytometry, microscopy or fluorimetry, and is proportional to the amount of dimers.

This technique has the unique capability to allow the simultaneous visualization of dimers and oligomers and larger aggregates in living cells, thus enabling the study of the process of aggregation from the first steps (Herrera & Fleming 2011).

BiFC assays have been developed with a wide range of fluorescent proteins, but probably the most popular for studies in mammalian cells is Venus, a third-generation yellow fluorescent protein. Venus is much brighter than other fluorescent proteins and has intrinsically improved folding efficiency at 37ºC, while most split fluorescent proteins need a preincubation at 30ºC (Herrera et al. 2012). It also enables the use of weaker promoters and thus approximates the expression of the interactors to physiological levels.

Some disadvantages of Venus-based BiFC systems include higher background and lower signal-to-noise ratios than the original proteins (GFP, YFP, EGFP, and EYFP) and saturated signals (Herrera et al. 2012; J. Y. Shyu et al. 2006). In order to overcome these disadvantages, split Venus halves have been intensively investigated, and some mutations and different split fragments have been found to reduce background and increase signal-to-noise ratio. To study protein interactions in Xenopus embryo, it was used a VN154 fragment carrying the T153M mutation (Saka et al. 2008). The pair used in a DJ1 BiFC system was the VN173/VC155 (Repici et al. 2013). A BiFC system for the study of c-Fos and c-Jun interaction used a VN155 and VC155 halves with 3 different point mutations V150A, L201V, and L207V (Nakagawa et al. 2011). Finally, splitting Venus at amino acid 210, instead of the most common 158 and 172 Aa split versions, leads to a striking decrease in background

fluorescence and a significant increase in the signal-to-noise ratio (Ohashi et al. 2012; Gookin & Assmann 2014).

2.Objectives

The main goal of this study is to develop a new cellular model for the visualization and study of GFAP oligomerization in living cells. We intend to create a set of BiFC plasmids with the GFAP gene fused to two complementary halves of the Venus fluorescent protein. We believe such a model would be extremely useful to characterize the intracellular pathways involved in normal and aberrant GFAP oligomerization and aggregation.

3. Materials and Methods

3.1- Materials

Cloning enzymes were acquired from Thermo Scientific (Waltham, United States) unless otherwise indicated. DNA purification kits, tryptone and T4 DNA ligase were purchased from NZYTech (Lisboa, Portugal). LB Agar and protease inhibitor cocktail were purchased from Amresco (Solon, United States). Dulbecco's Modified Eagle Medium (DMEM) and Phosphate buffer saline (PBS) without $Ca2^{+}$ or $Mg2^{+}$ were acquired from Lonza (Rockland, United States). Fetal bovine serum (FBS) was obtained from Biowest (Nuaillé, France). Fugene 6® transfection reagent was purchased from Promega (Madison, United States). Human glioblastoma U251 cells were obtained from Public Health England (Salisbury, United Kingdom). 25Q-Huntigtin-V2, 103Q-Huntigtin-V2, Tau-V2, and Syn – V2 plasmids were a kind gift from Tiago Outeiro (University of Göttingen, Germany). Plasmid DJ1-V2 was a kind gift from Flaviano Giorgini (University of Leicester, United Kingdom). The p53 – V2 and Mdm2 – V2 plasmids were a kind gift from Cecilia Rodrigues and Joana Amaral (University of Lisbon, Portugal) and the STAT3 – V2 plasmid was synthetized by Ana Maia at our laboratory (ITQB, Portugal).

3.2 - Generation of GFAP BiFC constructs.

Four different BIFC constructs were generated (Fig.12 A). These constructs encoded for GFAP fused to three different non-fluorescent halves of the Venus fluorescent protein: Venus 1, amino acids 1-210; a short version of Venus 2, amino acids 211-238; and a long version of Venus 2, amino acids 159-238. For the sake of simplicity, we will refer to Venus 2 (211-238) as S-Venus 2 and Venus 2 (159-238) as L-Venus 2 throughout the present thesis.

Fusion proteins were cloned in a pcDNA 3.1 backbone. In these constructs, the expression of fusion proteins was under the control of a cytomegalovirus promoter (pCMV), which allows high levels of constitutive expression in mammalian cells. After the insert, the vectors have a bovine growth hormone polyA tail for mammalian expression. Constructs have ampicillin and neomycin resistance sequences for selection in bacteria and mammalian cells, respectively. S-Venus 2 halves were inserted in the N- or C-termini of GFAP, L-Venus 2 in the C-terminal part of GFAP and Venus 1 in the N-terminus of GFAP. A fourth BiFC fusion gene was synthesized in a pcDNA 3.1 backbone, where S-Venus 2 was located in the C-terminus of GFAP.

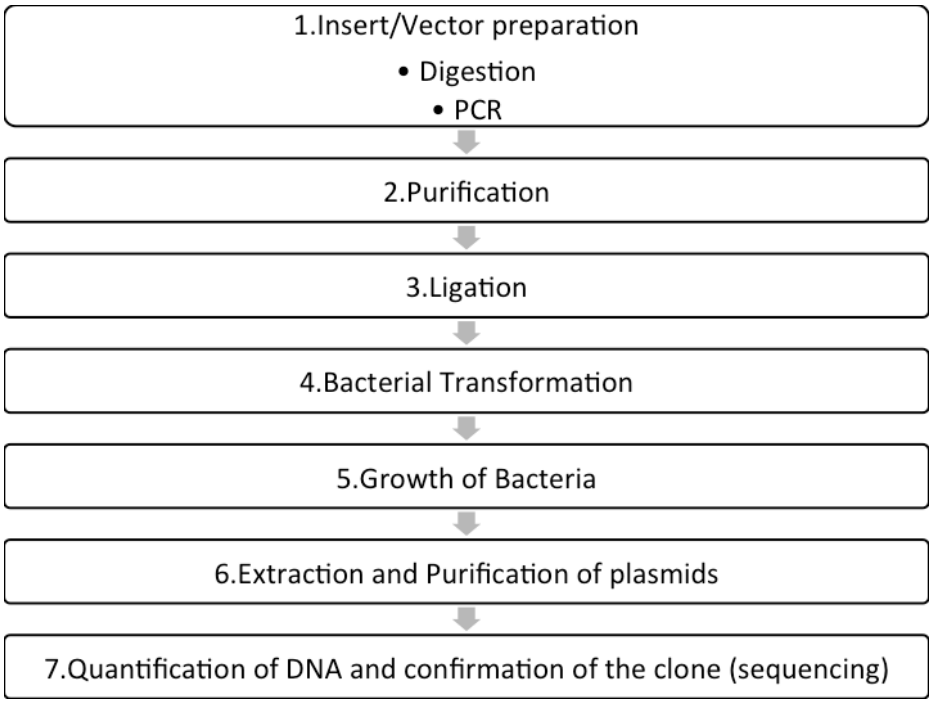

Figure 7 - Workflow to generate a BiFC construct.

3.2.1 - Insert/Vector preparation.

The Venus 1-GFAP was made using two cloning steps. First, Venus 1 was inserted in the pcDNA 3.1 vector. The Venus 1 insert was obtained by digestion of a previously synthesized gene with NheI and XbaI for 2 hours at 37 ºC. The pcDNA 3.1 vector was digested in the same conditions and incubated with alkaline phosphatase for 1 hour at 37 ºC to prevent unspecific religation of the vector. Insert and vector were then purified (Section 3.2.2 below) and ligated (Section 3.2.3 below).

A GFAP insert was obtained by PCR with the following primers:

GFAP Fwd – GCCGCTCGAGGAGAGGAGACGCATCACCTC

GFAP Rev - CTGAGGCGGATCCATCACATCACATCCTTGTGCTCC

A synthesized gene encoding for human GFAP was used as a template. The GFAP PCR product and the pcDNA-Venus 1 construct were digested with XhoI and BamHI for 2 hours at 37ºC and the vector was incubated with alkaline phosphatase for 1 hour at 37ºC to prevent background religation. Insert and vector were then purified (Section 3.2.2 below) and ligated (Section 3.2.3 below) to obtain the final Venus1-GFAP clones.

The pcDNA-S-Venus 2-GFAP construct was made by just one cloning step. The S-Venus 2-GFAP insert was obtained by digestion of a previously synthesized gene with BamHI for 2 hours at 37 ºC. The pcDNA 3.1 destination vector was digested in the same conditions and incubated with alkaline phosphatase for 1 hour at 37 ºC to prevent unspecific religation of the vector. Insert and vector were then purified (Section 3.2.2 below) and ligated (Section 3.2.3 below).

The pcDNA-GFAP-L-Venus 2 construct was also made by just one cloning step. GFAP was inserted in the pcDNA 3.1 vector carrying L-Venus 2. The GFAP insert was obtained by digestion of a previously synthesized gene with NheI and XhoI for 2 hours at 37 ºC. The pcDNA-L-Venus 2 destination vector was digested in the same conditions and incubated with alkaline phosphatase for 1 hour at 37 ºC to prevent unspecific religation of the vector. Insert and vector were then purified (Section 3.2.2 below) and ligated (Section 3.2.3 below).

3.2.2 – Purification

PCR products and digested vectors were run in agarose gels (1% in Tris-acetate-EDTA 1X) for 45 minutes to confirm the size of PCR products and digestion fragments, and the digestion efficiency. Selected bands were purified from gels by means of the NZYGelpure kit, following manufacturer´s instructions. First, agarose was melted at 60ºC for 10 minutes in 300 µl of Binding Buffer per 100 mg of Agarose. Second, melted agarose was added to a column and centrifuged at 13000xg for 1 min at RT. Third, columns were washed with an ethanol-based washing buffer. Finally, DNA was eluted with 30 µl of MiliQ water and quantified.

3.2.3 – Ligation

Once vector and insert were digested and purified, they were ligated using a T4 DNA ligase for 2 hours at room temperature. Four different proportions vector:insert were used to make sure the ligation succeeded: 1:0 (no insert), 1:3, 1:6 and 1:9. The 1:0 ligation was used as a control for non-specific vector religation. Ligations always contained 100 ng of vector and the amounts of insert were calculated accordingly.

3.2.4 – Bacterial Transformation

Thermocompetent *E. coli* bacteria were then transformed with ligation reactions. The ligation reaction was mixed with competent bacteria and incubated in ice for 30 minutes. Bacteria were heat-shocked at 42ºC for 45 seconds and placed in ice for 2 minutes. Three-hundred µl of liquid Luria Broth (LB) medium [1% w/v Tryptone; 0.5% w/v Yeast extract; 171 mM NaCl] without antibiotics were added, and bacteria were incubated in agitation (150 rpm) at 37ºC for 1 hour. Bacteria suspensions were seeded on LB Agar 1X petri dishes containing 100 µg/ml of ampicillin to select transformant clones and incubated at 37ºC overnight.

3.2.5 – Growth of Bacteria

Clones growing on LB-ampicillin plates should contain ligated plasmids, but these can contain the insert or not. In order to confirm that the clones carry the constructs of interest, 12 colonies were grown in liquid LB medium containing 100 µg/ml of ampicillin at 37ºC and in agitation (150 rpm) overnight.

3.2.6 – Extraction and Purification of Plasmids

In order to extract the constructs, bacteria were pulled down by centrifugation at 6000xg for 5 min at room temperature (RT), resuspended and lysed. After gentle centrifugation (13000xg 5 min at RT) to remove cell debris, clean supernatants were applied to DNA purification columns

from the NZYMiniprep kit. The columns were washed and the DNA was eluted in MiliQ H_2O and quantified. All the reagents were provided in the kit.

3.2.7 – Quantification of DNA and confirmation of clones by restriction reaction and sequencing

DNA was always quantified by means of a Nanodrop 2000c (Thermo Fisher Scientific Inc., West Palm Beach, United States). Clone confirmation was carried out by digestion 1-3 µg of DNA with the same restriction enzymes used for cloning. Digestion reactions were run in an Agarose gel (1% w/v) for 40 minutes at 80 volts. The clones showing a DNA fragment at the right size were sequenced for further confirmation (GATC, Cologne, Germany). Sequencing results were analyzed by means of the A Plasmid Editor (Ape) freeware (http://biologylabs.utah.edu/jorgensen/wayned/ape/). Positive clones were stored at -80ºC as glycerol stocks. Glycerol stocks were done by adding 500 µl of glycerol to 500 µl of bacteria suspension in LB liquid medium.

3.3 - Experiments in Mammalian Cells

Figure 8 - Schematic representation of transfection – Transfection mixture was done in microcentrifuge tubes, and the mixture was added to cells, which were seeded in different types of plates depending on the type of analyses.

GFAP-Venus BiFC constructs were tested for their behavior in cultured cells and compared with the behavior of BiFC systems previously developed. The experiments were carried out in human U251 glioma cells and HEK293 kidney cells, to compare the results obtained in cells expressing GFAP (U251) and cells lacking GFAP (HEK). Cells were transfected with different combinations of constructs, and analyzed 24 hours later by flow cytometry, fluorescence microscopy and western-blot to characterize and choose the best BiFC combination.

3.3.1 – Cell culture

HEK and U251 cells were maintained in DMEM supplemented with 10% FBS and 1% of penicillin/streptomycin commercial antibiotic mixture, at 37ºC and 5% CO2. Cells were always plated at a density of 10.000 cells/cm2 in order to obtain comparable results with different

techniques and plates and between experiments. Transfections were done using Fugene 6 in a proportion of 3:1 (µl of Fugene: µg of DNA). Fugene and DNA were mixed independently with 100 µl medium without serum or other additives and incubated for 5 minutes at room temperature. Fugene and DNA solutions were then mixed and incubated for 20 minutes before adding the transfection mixture to the plates. For 35 mm or 60 mm dishes, 65 µl or 130 µl of transfection mixture were added, respectively. Twenty-four hours after transfection, cells were processed specifically for each analytical method.

3.3.2 – Flow cytometry

Cells were seeded in 6-well plates. Cells were washed once with PBS and incubated with trypsin 0,25% for 5 min at 37ºC to detach cells from the substrate. Trypsin was neutralized with complete DMEM and cells were collected to sterile 15 ml tubes. Cells were centrifuged at 300xg for 5 min, the supernant was removed, and cells were resuspended in 500 µl of PBS. Ten thousand cells per experimental group were analyzed by means of a FACSCalibur flow cytometer equipped with a low-power aircooled 15mW blue laser (488nm) argon laser and a red (635nm) diode laser (band-pass filter 530/30). Data were analyzed and represented by means of FlowJo software (Tree Star Inc., Ashland, United States).

3.3.3 – Microscopy

Cells were seeded in 35mm glass-bottom plates. Images were acquired on a custom-built Nikon Eclipse TE2000-S equipped with a Hamamatsu Flash 2.8 sCMOS camera and DAPI + GFP fluorescence filter sets, and controlled with the MicroManager v4.1.14 software. Pictures were taken using the 100X objective and analyzed by means of the ImageJ free online software (http://rsbweb.nih.gov/ij/).

3.3.4 – Protein extraction

Cells were washed once with PBS, and then lysed with a lysis buffer (NaCl 150mM, NP-40 1%, Tris-Cl 50mM ph 8.0) containing protease inhibitors. Cells were scrapped directly from the plates, transferred to microcentrifuge tubes, and incubated in ice for 10 min. Cells were sonicated for 5 seconds by means of a Sonifier W-450 D sonicator (Emerson, Danbury, United States) to disrupt the membranes and release intracellular proteins, allowing their isolation and detection by western blotting. To avoid protein degradation by cell proteases, cells were always kept in ice during extraction procedures. Protein concentration was quantified on a microplate reader (Multiskan Go, Thermo Scientific, Waltham, United States) by means of the Bradford method. Briefly, 2 µl of protein sample were added to 200 µl of the Bradford reagent and

incubated for 10 minutes, and their absorbance was measured at 595 nm. Protein concentrations were calculated by means of a standard curve produced from known concentrations of albumin (0.125 to 2 μg/μl).

3.3.5 – Western Blot

Twenty μg of protein were mixed with 4x denaturing loading buffer (1 M Tris pH 7; 8% SDS; 40% glycerol; 6.3% β-mercaptoethanol; bromophenol blue), boiled at 95ºC for 5 min, and incubated at 4ºC for 5 min. Protein samples were run in SDS-PAGE 10% (w/v) Acrylamide gels made with Protogel reagents (United Diagnostics, Atlanta, United States). Samples were run at 125V for 60 min and transferred to a nitrocellulose membrane at 100V for 60 minutes. Membranes were stained with Ponceau S 0.1% (w/v) to verify protein transfer efficiency as well as equal sample loading. Membranes were washed with miliQ water and Tris-HCl buffer saline (TBS, 150 mM NaCl, 50 mM Tris pH 7.4) and blocked with 5% (w/v) non-fat dry milk in TBS for 1 hour at room temperature in agitation. Membranes were washed 3 times with TBS-Tween (0.05% v/v) and incubated with the following antibodies overnight at 4ºC in agitation: a Rabbit polyclonal anti-GFAP antibody (1:1000, Millipore, Billerica, United States of America) or a mouse monoclonal anti-GAPDH antibody (1:1000, Ambion, West Palm Beach,

United States). Primary antibodies were diluted in 5% (w/v) bovine serum albumin (BSA) in TBS and sodium azide 0.02% (w/v) to prevent contaminations. Membranes were then washed 3 times for 10 min each with TBS-T and incubated with anti-Rabbit and Mouse horseradish peroxidase-conjugated secondary antibodies (GE-Healthcare, Little Chalfont, United Kingdom) for 2 hours in agitation at room temperature. Secondary antibodies were diluted at a 1:1000 concentration in 5% (w/v) non-fat dry milk. Membranes were washed 3 times for 10 min each with TBS-T, incubated with chemiluminescent HRP reagents (Millipore, Billerica, United States), and imaged by means of a Chemidoc device (XRS+, Biorad, California, United States).

4-Results

4.1-Production of GFAP-Venus BiFC constructs.

BiFC systems are composed of two constructs, where the proteins of interest are fused either to the N-terminal half of Venus (Venus 1) or the C-terminal half of Venus (Venus 2). Venus halves can have different sizes (Kodama & Hu 2010; Y. J. Shyu et al. 2006; Nakagawa et al. 2011; J. Y. Shyu et al. 2006). The most common combinations are Venus 1(1-158)/Venus 2(158-238), and Venus 1(1-172)/Venus 2 (158-238), but the combination with the lowest background and highest signal-to-noise ratio is Venus 1(1-210)/Venus 2(210-238) (Ohashi et al. 2012). We tested this combination and a Venus 1(1-210)/Venus 2(158-238) combination (Figure 8), which was also reported to work but with lower signal-to-noise ratio. Venus halves can be located in the N-terminus or the C-terminus of the proteins of interest, and this must be tested empirically, as it is not possible to predict the best combination of BiFC constructs based on the sequence. There were reports indicating that intermediate filaments do not behave normally when they had tags in their C-terminal region (Tang et al. 2006), so priority was given to tags located in the N-terminus of GFAP. However, two anti-parallel combinations were also tested (Fig. 8).

The GFAP-S-Venus2 fusion gene was synthesized, but the others were produced in our laboratory as follows.

4.1.1 – Production of the Venus 1 (1-210)-GFAP construct

The pcDNA-Venus 1 (1-210)-GFAP construct was made using two subcloning steps. First, Venus 1 (1-210) was inserted in a pcDNA3.1 vector to allow us to express the fusion proteins in mammalian cells. Venus 1 was released from a plasmid by digestion with NheI and XbaI, and pcDNA3.1 was digested with the same enzymes to generate cohesive ends that allowed the ligation of insert and vector. Figure (9) B shows some positive clones from the ligation. Plasmids extracted from individual colonies were digested with NheI and XbaI to release the insert. Venus 1 has 210 amino acids, so the excised band should have approximately 630 bp.

Second, the human GFAP sequence was PCR-amplified and inserted in the pcDNA-Venus1 construct. GFAP-specific primers carrying BamHI and XhoI restriction sites were used to amplify human GFAP. The PCR product and the destination vector were digested with BamHI and XhoI, ligated and transformed into bacteria. Figure (9) C shows positive clones carrying the constructs of interest, as determined by digestion with

BamHI and XhoI. GFAP has 432 amino acids, so the corresponding band should have approximately 1300 bp.

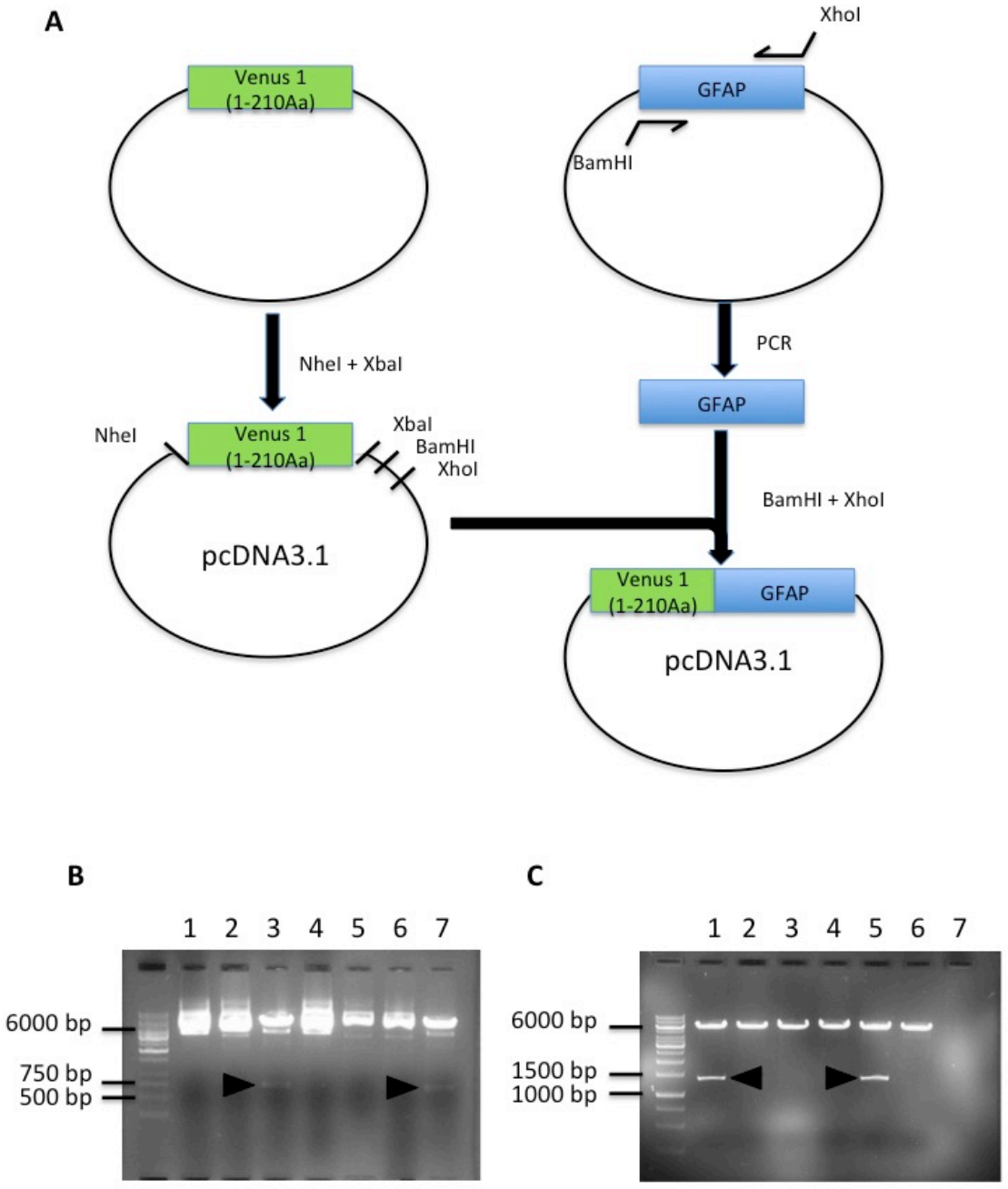

Figure 9 . Schematic diagram showing the different steps to obtain the Venus 1-GFAP plasmid in pcDNA3.1. A) A plasmid carrying Venus 1 (1-210) in a pcDNA 3.1 backbone was produced, and used as a destination vector for GFAP. GFAP was amplified by PCR from a synthetic template. Both vector and insert were digested with BamHI and XhoI and ligated to produce the final pcDNA-Venus1(1-210)-GFAP plasmid. B) Test digestion of clones with pcDNA3.1 with Venus 1 (1-210 A.a – 630 bp) (arrow head – positive clones). C) Test digestion of pcDNA-Venus 1 (1-210)-GFAP (arrowhead – positive clones)

4.1.2 - Production of the S-Venus 2/GFAP constructs

The S-Venus 2-GFAP construct was made by one cloning step. It was subcloned in the pcDNA 3.1 vector to allow us to express the S-Venus2-GFAP fusion in mammalian cells. The S-Venus 2-GFAP insert was obtained by BamHI digestion of a previously ordered plasmid. The pcDNA 3.1 vector was also digested with BamHI to get cohesive ends.

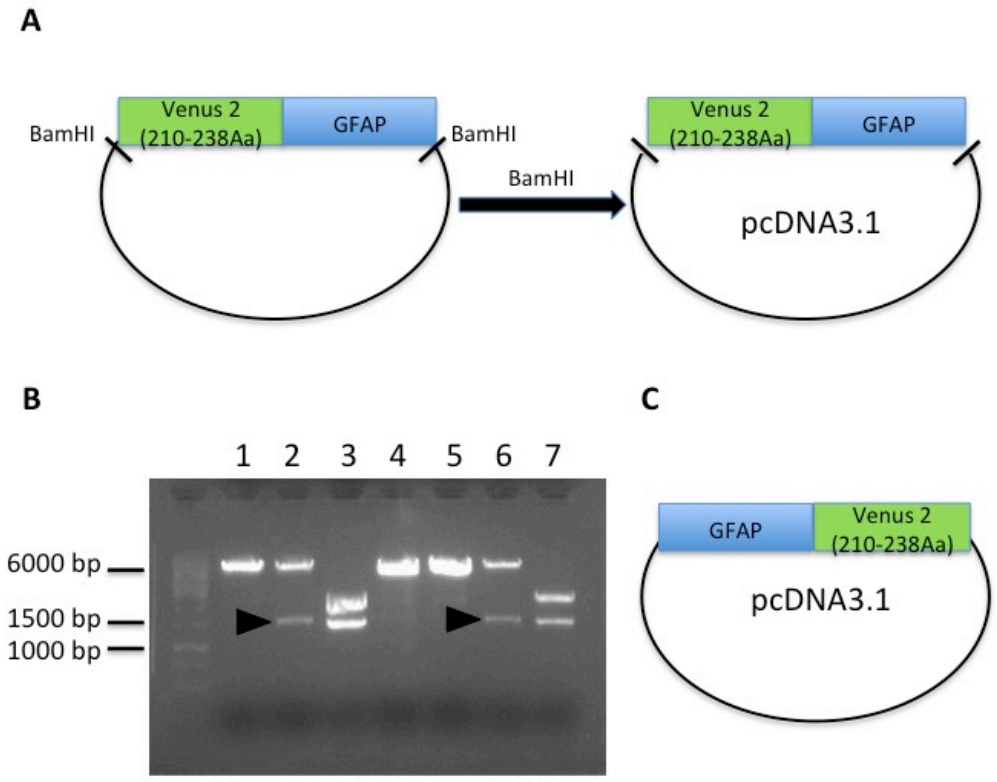

Figure 10 - Schematic diagram showing the two different plasmids carrying S-Venus 2 – GFAP fusion genes in pcDNA3.1. S-Venus 2 (210-238) was located in the N- or the C-terminus of GFAP. A) A plasmid carrying the fusion Venus 2(210-238)-GFAP was ordered, and the fusion protein was subcloned in a pcDNA3.1 vector for mammalian expression. B) Test digestion of clones carrying the S-Venus 2-GFAP fusions (arrowhead – positive clones). C) A plasmid carrying the GFAP-S-Venus2 fusion was synthesized directly in the pcDNA3.1 mammalian expression vector.

Vector and insert were purified and ligated to originate the final pcDNA-S-Venus 2-GFAP construct (Fig. 10 – A). Fig 10 – B shows the BamHI digestion to identify positive clones, which should release an insert of around 1400 bp.

4.1.3 – Production of the GFAP-Venus 2 (158-238).

The GFAP-L-Venus 2 was made by substituting huntingtin exon 1 by human GFAP in a BiFC construct previously developed by Dr. Herrera. The GFAP insert was obtained by digestion of our pcDNA-GFAP-S-Venus2 plasmid with NheI and XhoI. The pcDNA-Htt-L-Venus 2 vector was also digested with NheI and XhoI in order to obtain cohesive ends and thus facilitate the ligation of vector and insert (Fig 11 – A). Fig 11 – B shows the digestion test with NheI and XhoI to identify the positive clones, which should release an insert of approximately 1300 bp.

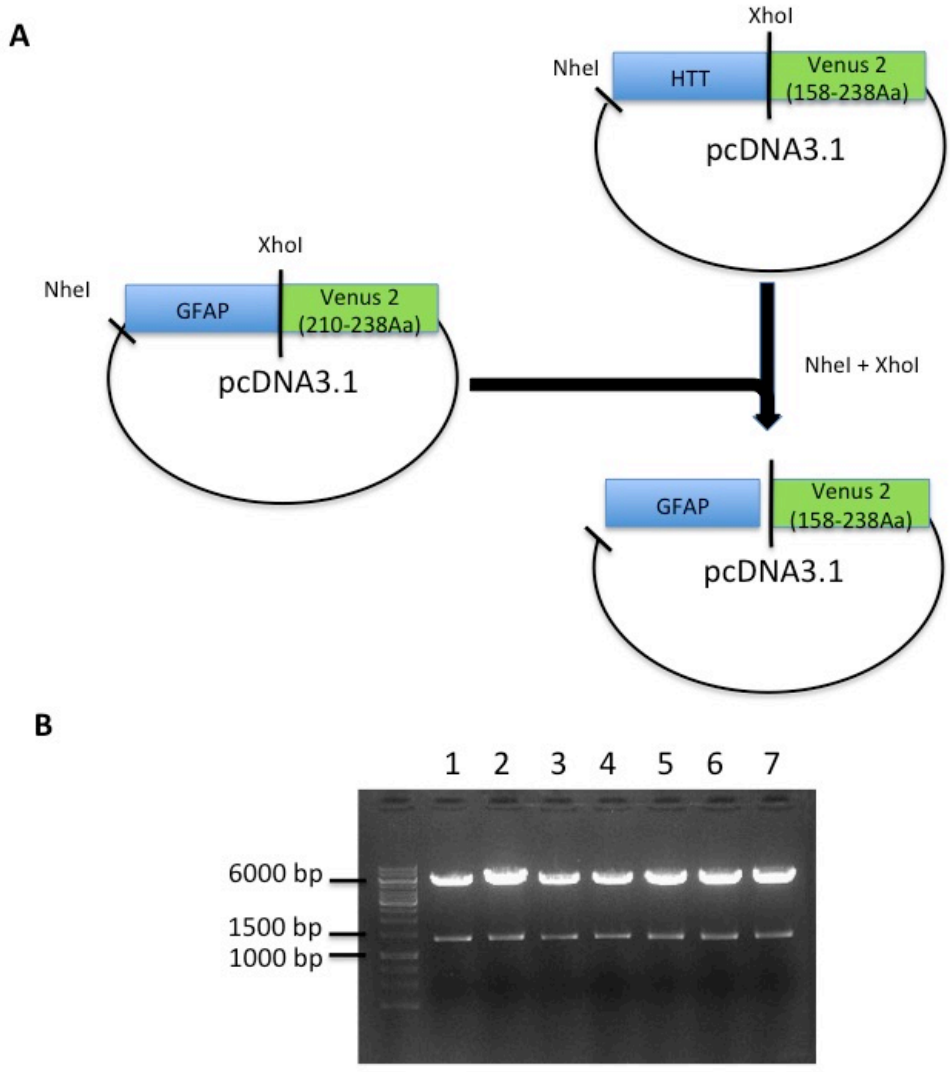

Figure 11 - Schematic diagram showing the different steps to obtain The GFAP-L-Venus 2 plasmid – A) Huntingtin exon 1 (Htt) sequence was removed from a BiFC plasmid previously developed in Dr. Outeiro´s laboratory and substituted by GFAP. GFAP was digested from the GFAP-S-Venus2 construct described above. B) Test digestion of positive clones carrying pcDNA-GFAP-L-Venus 2. The right insert size (1296bp) is indicated by the arrowhead.

4.2-Fluorescence levels of BiFC pairs and pattern of aggregation in V1-GFAP/GFAP-L-V2

We tested three different combinations of GFAP-Venus BiFC constructs. All of them included the Venus 1 – GFAP construct paired with the different Venus 2 – GFAP constructs (Fig 12 - A).

Cells transfected with different BiFC pairs were analyzed by Flow cytometry (Fig 12 B and C). Only one BiFC pair, Venus 1–GFAP/GFAP–L-Venus 2, produced fluorescence. However, it had low fluorescence in comparison with the Htt-Venus BiFC system (Herrera et al. 2011)

Western Blot analysis confirmed that transfected HEK cells expressed BiFC constructs (Fig 12 D). HEK cells do not express endogenous GFAP, which allowed easy detection of the fusion proteins with an anti-GFAP antibody. GFAP has a molecular weight of 50 KDa, and the molecular weight of the different fusion proteins was consistent with their tags. Venus has a molecular weight of 27 KDa, Venus 1 is between 2/3 and ¾ of Venus and Venus 2 is approximately 1/3-1/4 of Venus. Obviously, there are no differences in molecular weight if the tag is located in the N- or the C-terminus of GFAP (Fig 12 – B).

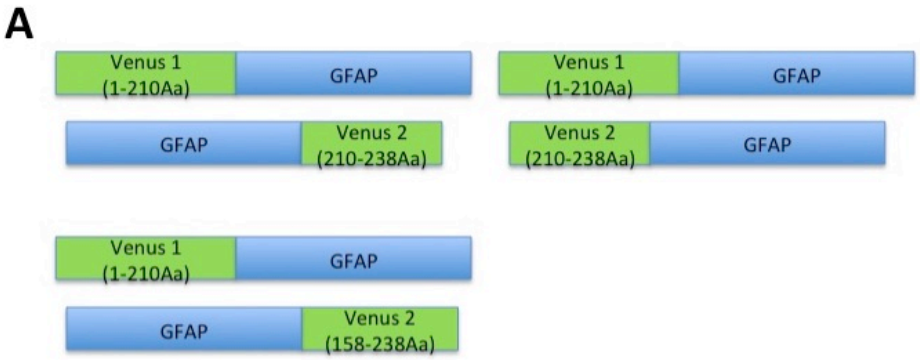
A
Venus 1 (1-210Aa)
GFAP
GFAP
Venus 2 (210-238Aa)
Venus 1 (1-210Aa)
GFAP
Venus 2 (210-238Aa)
GFAP
Venus 1 (1-210Aa)
GFAP
GFAP
Venus 2 (158-238Aa)

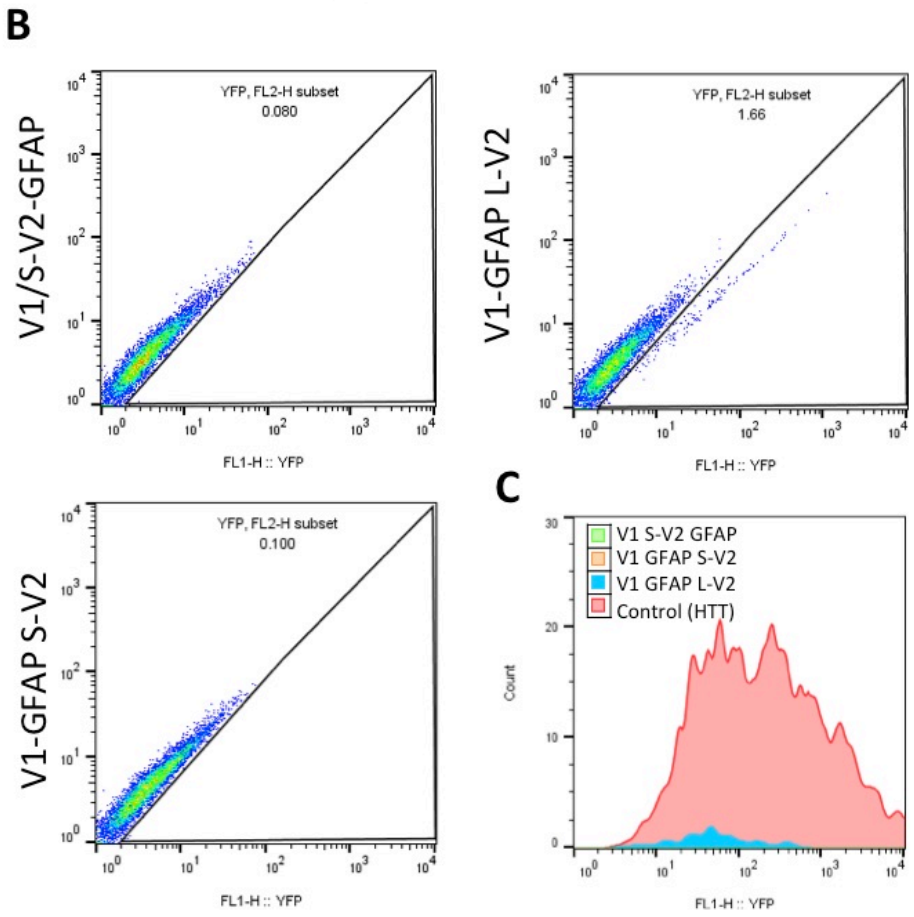
B
V1/S-V2-GFAP
YFP, FL2-H subset
0.080
FL1-H :: YFP
V1-GFAP L-V2
YFP, FL2-H subset
1.66
FL1-H :: YFP
V1-GFAP S-V2
YFP, FL2-H subset
0.100
FL1-H :: YFP
C
V1 S-V2 GFAP
V1 GFAP S-V2
V1 GFAP L-V2
Control (HTT)
Count
FL1-H :: YFP

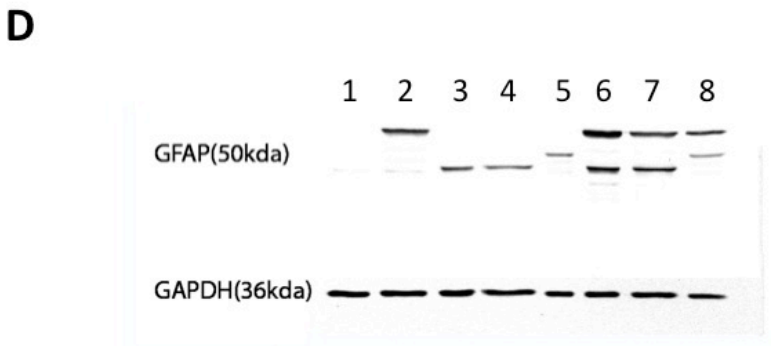
D
1 2 3 4 5 6 7 8
GFAP(50kda)
GAPDH(36kda)

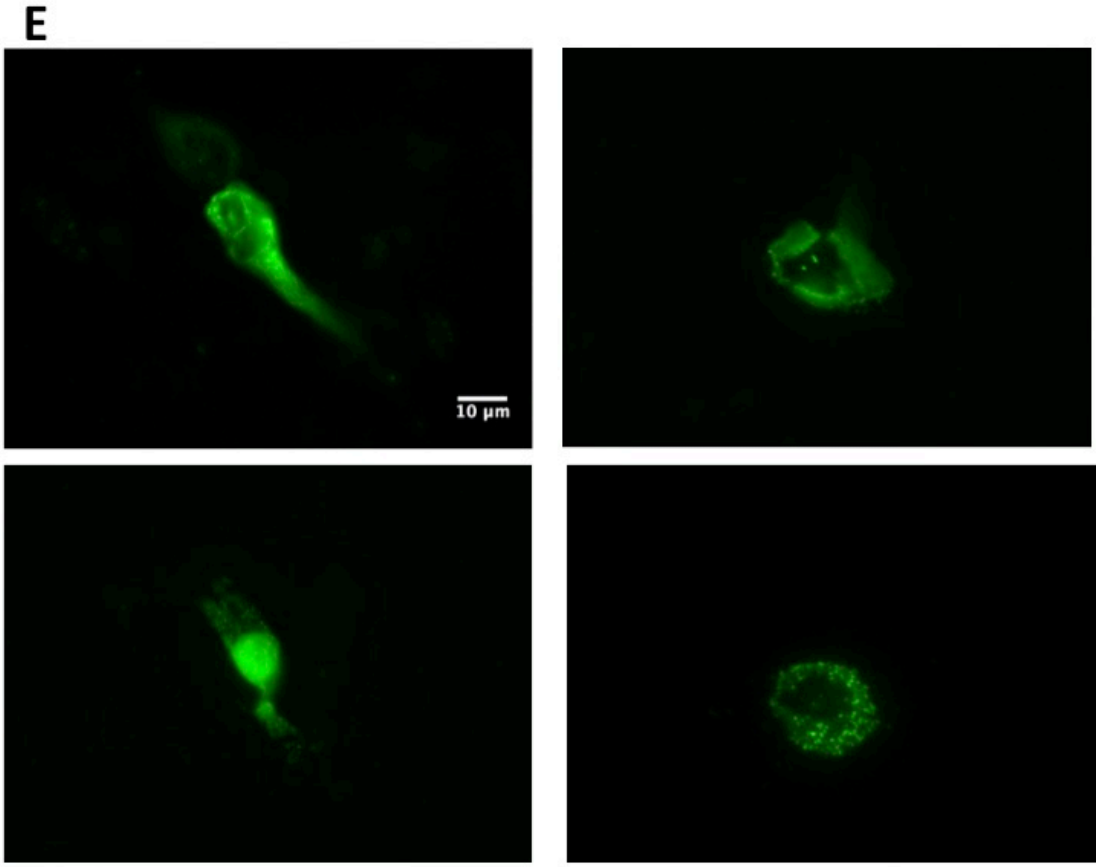

Figure 12 – BiFC pairs show low fluorescence levels. A) Cells were transfected using three different combinations of BiFC constructs. B) Only the Venus 1–GFAP/GFAP – L-Venus 2 combination showed some fluorescence, as determined by Flow Cytometry. C) Fluorescence is always lower than the signal from the Huntigtin BiFC pair previously developed by Dr. Herrera. D) Immunoblots show that GFAP-Venus fusion proteins are expressed in transfected HEK cells. Lanes: 1) Control, 2) Venus 1 GFAP, 3) S-V2-GFAP, 4) GFAP–S-V2, 5) GFAP–L-V2, 6) Venus 1–GFAP/S-V2-GFAP, 7) Venus 1–GFAP/GFAP–S-V2, 8) Venus 1–GFAP/GFAP–L-V2. E) HEK cells transfected with the Venus 1–GFAP/GFAP – L-Venus 2 combination show aberrant patterns of intracellular distribution. Scale bar 10 µm.

Microscopy results were consistent with flow cytometry (Fig 12-E). Only the V1-GFAP/GFAP-L-V2 pair produced fluorescence, but it labeled a very a low number of cells. Furthermore, most labeled cells did not show GFAP fibers, but a cytoplasmic signal with a rather heterogeneous distribution. Rosenthal fibers or clear aggregation patterns

were not observed, but the signal did not delineate the regular intermediate filament network.

4.3- Interactions of GFAP with other proteins related to neurodegeneration

Next, we asked whether GFAP interacted with other proteins and also produced a pattern of aggregation. HEK cells were transfected with the Venus 1–GFAP plasmid in combination with other plasmids carrying proteins related to neurodegeneration fused to the L-Venus 2 tag. One group of these proteins is directly involved in neurodegenerative diseases, has a strong tendency to aggregation and is localized mainly in the cytosol. These include huntingtin, tau, synuclein and DJ-1. The other group of proteins is mostly composed transcription factors (STAT3 and p53) or their regulators (mdm2), usually does not produce aggregates and its localization shifts between nuclear and cytosolic. The combination of GFAP with other aggregation-prone proteins produces higher levels of fluorescence than its combination with proteins from the second group (Fig. 13 A).

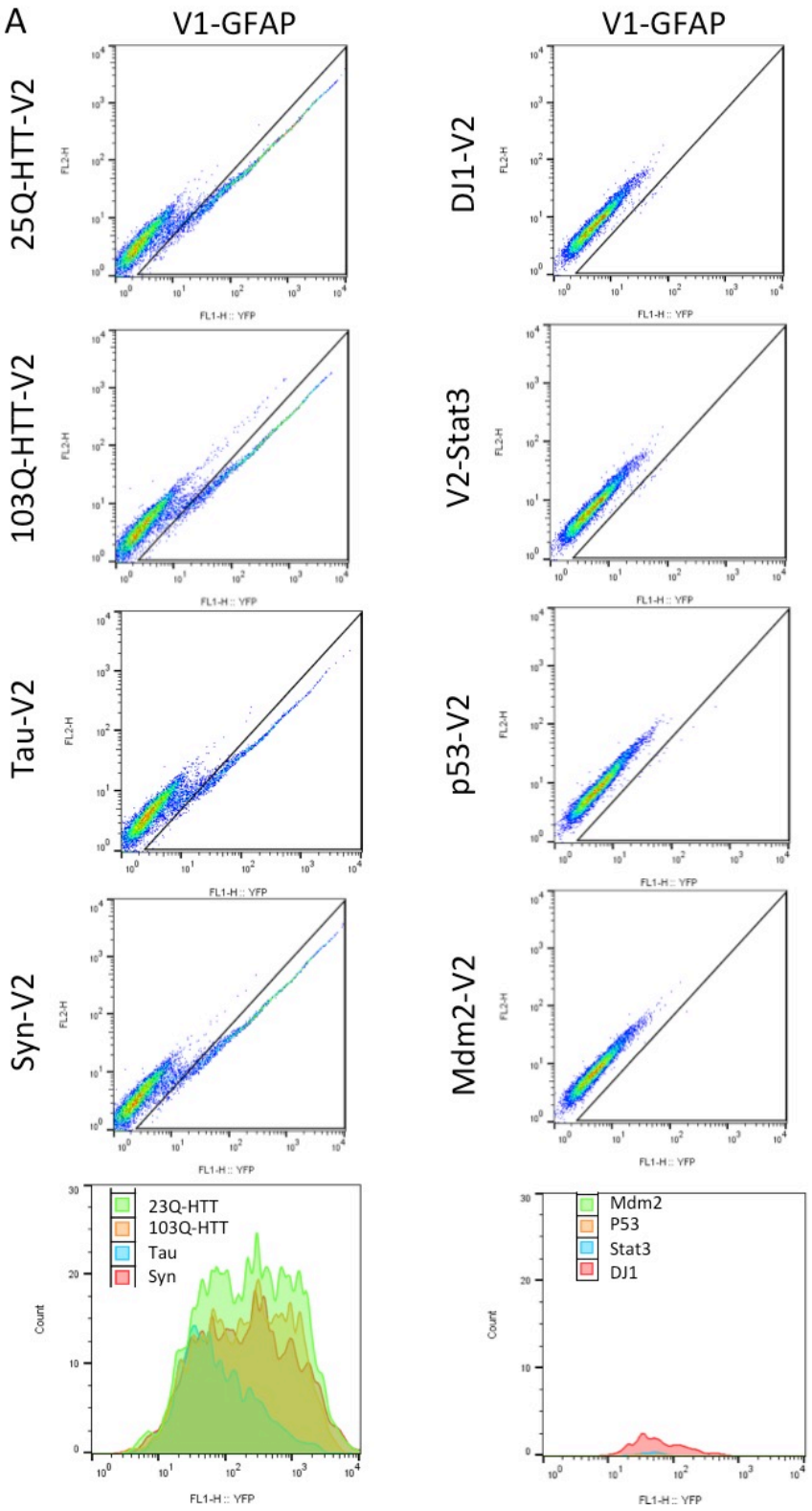
A
V1-GFAP
V1-GFAP
25Q-HTT-V2
DJ1-V2
103Q-HTT-V2
V2-Stat3
Tau-V2
p53-V2
Syn-V2
Mdm2-V2
FL2-H
FL1-H :: YFP
Count
23Q-HTT
103Q-HTT
Tau
Syn
Mdm2
P53
Stat3
DJ1

B

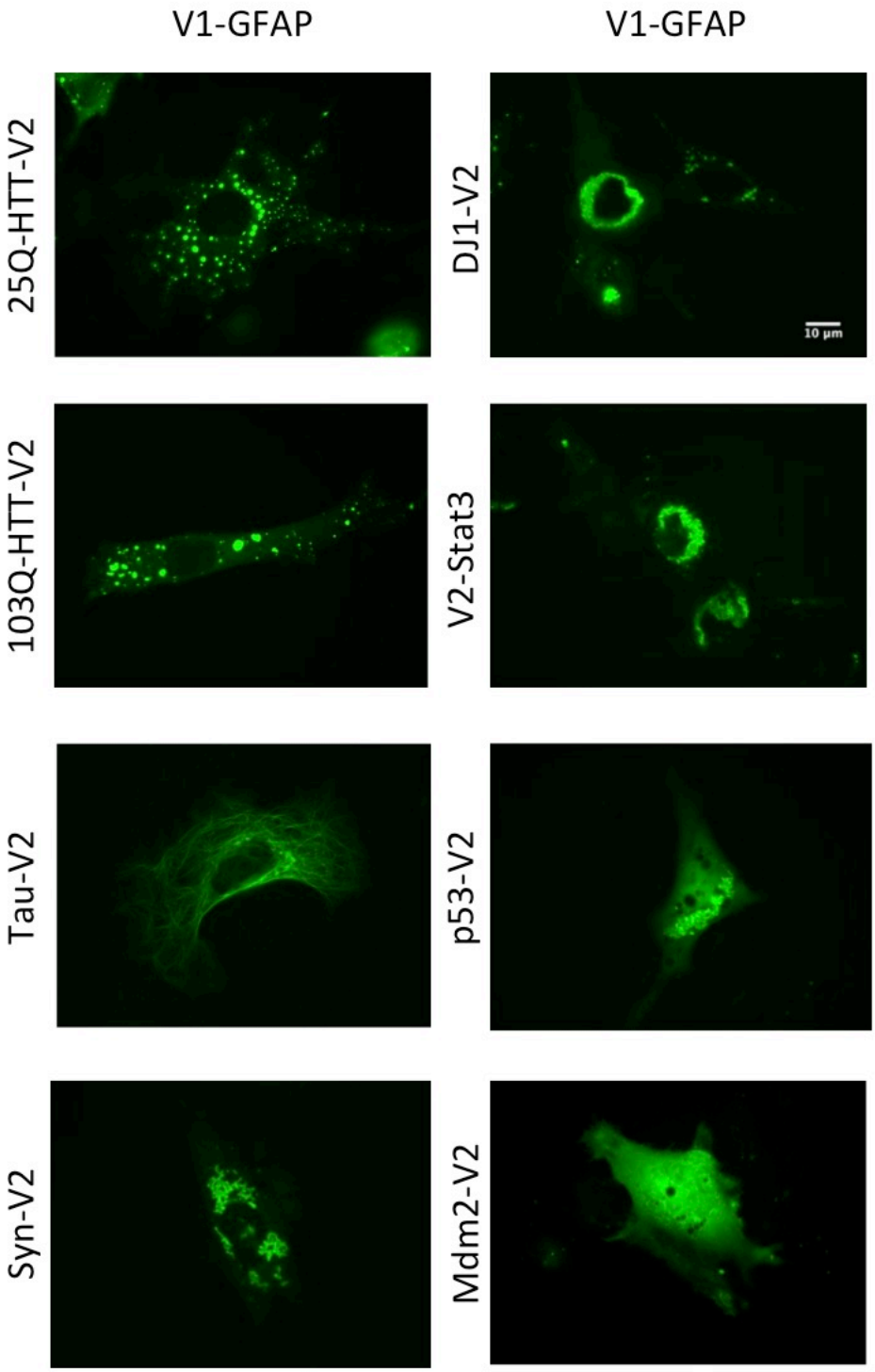

Figure 13 – Interaction between GFAP and other proteins related to neurodegeneration. A) Flow cytometry charts of different pairs of BiFC constructs. Cytosolic aggregation-prone proteins produced more signal. B) Representative microscopy images of the interactions between the Venus 1 GFAP and the other proteins tagged with Venus 2.

GFAP-Venus BiFC pairs showed an aberrant cytoplasmic distribution (Fig. 12 E), but the interactions between GFAP and the tested proteins produced completely different patterns of aggregation and distribution. GFAP/HTT pairs showed spherical aggregates in the cytosol, resembling HTT aggregates in a similar BiFC system (Herrera & Fleming 2011). GFAP/103QHTT seemed to produce bigger aggregates than the GFAP/25QHTT pair, but we would need to increase the number of experiences and make quantitative analyses to draw any definitive conclusions. The Tau/GFAP pair has the same appearance as the corresponding Tau/Tau BiFC system. Tau is a microtubule-binding protein and therefore it delineates the microtubular network. No aggregates were observed in this case, indicating that GFAP does not necessarily aggregate, and that its abnormal distribution may depend on the intracellular context. Syn, DJ-1, p53 and stat3 formed large aggregates surrounding the nucleus when they were combined with GFAP. Syn/syn, DJ-1/DJ-1, p53/p53, p53/mdm2 and STAT3/STAT3 BiFC systems did not produce aggregates (Dias et al. 2013; Sajjad et al. 2014), indicating that GFAP can induce the aggregation of particular proteins. Finally, the combination GFAP/mdm2 produced homogeneous fluorescence distributed throughout the nucleus and the cytoplasm, and no aggregates. These results suggest that GFAP behavior does not depend only on the tag, but also on the intracellular context.

5.Discussion

In the present work we tried unsuccessfully to generate a BiFC system to study GFAP oligomerization in living cells. However, we are still trying to generate the system because of all the study possibilities that he will offer. Astrocytes play a major role in the response to injury of CNS, and GFAP is the principal component of astroglial filaments, relevant in their response to injury (Eng et al. 1971; Carmen et al. 2007). GFAP mutations are responsible for Alexander Disease (Yoshida et al. 2011), leading to GFAP aggregation in Rosenthal Fibers and neurodegeneration (Quinlan et al. 2007). Finally, GFAP has an important role in astroglial proliferation and its expression is correlated with lower malignancy of gliomas (Seri et al. 2001; Garcia et al. 2004). However, there is no method to analyze GFAP behavior in living cells.

Current evidence indicates that oligomers are more toxic than large aggregates in PD and AD, and there is one report indicating the same in Alexander disease. A BiFC model for GFAP would shed some light on this subject, allowing us to visualize GFAP oligomerization in normal and and pathological conditions. Furthermore, it would allow us to study GFAP interactions with other proteins in living cells. The modulation of this filament´s interactions can lead to novel and interesting approaches to

treat not only neurodegenerative diseases but other insults like ischemic stroke (De Pablo et al. 2013).

BiFC systems have to be built empirically, as it is impossible to predict the right combination of constructs a priori. There are BiFC systems generated for many proteins, but there is no a single formula that fits all. Aggregation of mutant huntigtin was studied adding the Venus halves to the C-terminus of the huntigtin protein (Herrera et al. 2011). For the alpha-synuclein BiFC system, the venus 1 half was inserted in the N-terminus of synuclein, while the venus 2 half was inserted in the C-terminus (Outeiro et al. 2008). In the DJ1 BiFC system, Venus 1 and Venus 2 halves were added to the C-terminus of DJ1 but with a linker (Repici et al. 2013). We initially tried to insert both Venus 1 and Venus 2 halves in the N-terminus of GFAP, as Dr. Michel Brenner warned us that a tag in the tail region of GFAP could lead to aggregation. However, we obtained no fluorescence, probably due to the version of Venus fragments used (1-210), rather than the position of the tag. We will next try with the 1-158 partition.

We tried to fuse GFAP to a novel partition of Venus (1-210;210-238). BiFC systems have disadvantages like higher background, lower signal-to-noise ratios and saturated signals (Herrera et al. 2012; J. Y. Shyu et al. 2006). To overcome these disadvantages, a new split of Venus (in A.a 210) was previously tested and lead to better signal-to-noise ratios

(Ohashi et al. 2012). We failed to obtain signal with this split venus system. Ohashi et al. (2012) used this version to study the interaction between cofilin and actin, with a configuration similar to the one we used in this work. Further studies should be done to confirm that this split version actually works in different experimental conditions.

The combination Venus 1 1-210, Venus 2 158-210 produced fluorescence but the intracellular distribution was anomalous. This is consistent with previous papers stating that GFAP can tolerate the incorporation of a tag but with consequences for filament organization (Perng et al. 2008). However, when GFAP was combined with other proteins, GFAP did not aggregate, so the effect of tags could be context-dependent.

In terms of future perspectives, we need to try the remaining combination of Venus constructs. Until now we only changed the position of Venus 2, so we will insert Venus 1 in the C-terminus of GFAP and pair it with Venus 2 halves in the C- an N-terminus. We could also try to add a linker between Venus halves and GFAP to provide some flexibility. Bearing in mind that the Head and Tail domains of GFAP can have a very important role in its normal oligomerization, we could try to tag GFAP within its coding sequence. It is now possible to create functional fluorescent fusion proteins by random insertion of GFP with an in vitro transposition reaction. This idea was tested in a glutamate receptor

subunit, GluR I, and the G protein subunit, α_s (Sheridan et al. 2002). Thus, we will try to do a random insert of Venus halves in GFAP and analyze if these tags actually perturb normal oligomerization of GFAP and the formation of filaments.

6.Conclusions

In the present study, we failed to develop a BiFC system for the visualization and study of the intermediate filament GFAP, and we can conclude that:

1) The Venus 1-210/Venus 210-238 BiFC pair is not functional, at least in the context of the GFAP protein.
2) The V1 (1-210)-GFAP and GFAP-V2(159-210) pair is functional but does not reproduce the normal intracellular distribution of GFAP.
3) Tagged GFAP can co-aggregate selectively with various aggregation-prone and neurodegeneration-related proteins.

Further studies with all the combinations of V1 and V2 with different sizes in both sides or within GFAP are needed to know if a BiFC system for GFAP or other intermediate filaments is actually possible.

7.References

Alexander, W.S., 1947. PROGRESSIVE FIBRIXOID DEGENERATION OF FIBRILLARY ASTROCVTES ASSOCIATED WITH MENTAL RETARDATION IN A HYDROCEPHALIC INFANT 1 IN the following case of progressive hvdrocephalus in an infant , the brain displays on histological examination a type of degenerat. , pp.373–381.

Bachetti, T. et al., 2012. Beneficial effects of curcumin on GFAP filament organization and down-regulation of GFAP expression in an in vitro model of Alexander disease. *Experimental cell research*, 318(15), pp.1844–54. Available at: http://www.ncbi.nlm.nih.gov/pubmed/22705585 [Accessed September 16, 2014].

Back, S.A. et al., 2005. Hyaluronan accumulates in demyelinated lesions and inhibits oligodendrocyte progenitor maturation. *Nature Medicine*, 11(9), pp.966–972. Available at: http://www.nature.com/doifinder/10.1038/nm1279.

Bianchini, D. et al., 1992. GFAP expression of human Schwann cells in tissue culture. *Brain research*, 570(1-2), pp.209–17. Available at: http://www.ncbi.nlm.nih.gov/pubmed/1617413.

Blechingberg, J. et al., 2007. Identification and characterization of GFAPkappa, a novel glial fibrillary acidic protein isoform. *Glia*, 55(5), pp.497–507.

Bongcam-Rudloff, E. et al., 1991. Human Glial Fibrillary Acidic Protein: Complementary DNA Cloning, Chromosome Localization, and Messenger RNA Expression in Human Glioma Cell Lines of Various Phenotypes. *Cancer research*, 51(5), pp.1553–1560.

Brenner, M. et al., 1994. GFAP promoter directs astrocyte-specific expression in transgenic mice. *The Journal of neuroscience : the official journal of the Society for Neuroscience*, 14(3 Pt 1), pp.1030–1037.

Brenner, M. et al., 2001. Mutations in GFAP, encoding glial fibrillary acidic protein, are associated with Alexander disease. *Nature genetics*, 27(1), pp.117–120.

Carmen, J. et al., 2007. Revisiting the astrocyte-oligodendrocyte relationship in the adult CNS Revisiting the astrocyte – oligodendrocyte relationship in the adult CNS. *Progress in Neurobiology*, 82(March), pp.151–162.

Carotti, S. et al., 2007. Glial Fibrillary Acidic Protein as an Early Marker of Hepatic Stellate Cell Activation in Chronic and Posttransplant Recurrent Hepatitis C. *Liver Transplantation*, 13(3), pp.465–466.

Chen, Y. et al., 2011. Alexander disease causing mutations in the C-terminal domain of GFAP are deleterious both to assembly and network formation with the potential to both activate caspase 3 and decrease cell viability. *Experimental Cell Research*, 317(16), pp.2252–2266. Available at: http://dx.doi.org/10.1016/j.yexcr.2011.06.017.

Dias, J. et al., 2013. Live-cell imaging of p53 interactions using a novel Venus-based bimolecular fluorescence complementation system.

Eliasson, C. et al., 1999. Intermediate Filament Protein Partnership in Astrocytes. *The Journal of Biological Chemistry*, 274(34), pp.23996–24006.

Eng, L.F. et al., 1971. An acidic protein isolated from fibrous astrocytes. *Brain research*, 28(2), pp.351–354.

Fletcher, D.A. & Mullins, R.D., 2010. Cell mechanics and the cytoskeleton. *Nature*, 463(7280), pp.485–492.

Garcia, a D.R. et al., 2004. GFAP-expressing progenitors are the principal source of constitutive neurogenesis in adult mouse forebrain. *Nature neuroscience*, 7(11), pp.1233–41. Available at: http://www.ncbi.nlm.nih.gov/pubmed/15494728 [Accessed August 29, 2014].

Geisler, N. & Weber, K., 1983. Amino acid sequence data on glial fibrillary acidic protein (GFA); implications for the subdivision of intermediate filaments into epithelial and non-epithelial members. *The EMBO journal*, 2(11), pp.2059–63. Available at: http://www.pubmedcentral.nih.gov/articlerender.fcgi?artid=555409&tool=pmcentrez&rendertype=abstract.

Gomi, H. et al., 1995. Mice devoid of the glial fibrillary acidic protein develop normally and are susceptible to scrapie prions. *Neuron*, 14(1), pp.29–41.

Gookin, T.E. & Assmann, S.M., 2014. Significant reduction of BiFC non-specific assembly facilitates in planta assessment of heterotrimeric G-protein interactors. *The Plant journal : for cell and molecular biology*, 80(3), pp.553–67. Available at: http://www.pubmedcentral.nih.gov/articlerender.fcgi?artid=4260091&tool=pmcentrez&rendertype=abstract.

Gunning, P.W. et al., 2015. The evolution of compositionally and functionally distinct actin filaments. *Journal of cell science*, 128(11), pp.2009–2019. Available at: http://jcs.biologists.org/content/128/11/2009.long.

Halassa, M.M., Fellin, T. & Haydon, P.G., 2007. The tripartite synapse: roles for gliotransmission in health and disease. *Trends in molecular medicine*, 13(2), pp.54–63.

Herrera, F. et al., 2011. Visualization of cell-to-cell transmission of mutant huntingtin oligomers. *PLoS Currents*, 3, p.RRN1210. Available at: http://eutils.ncbi.nlm.nih.gov/entrez/eutils/elink.fcgi?dbfrom=pubmed&id=21331289&retmode=ref&cmd=prlinks\npapers2://publication/doi/10.1371/currents.RRN1210.

Herrera, F. & Fleming, T., 2011. a -Synuclein modifies huntingtin aggregation in living cells. *FEBS LETTERS*. Available at: http://dx.doi.org/10.1016/j.febslet.2011.11.019.

Herrera, F., Gonçalves, S. & Outeiro, T.F., 2012. Imaging Protein Oligomerization in Neurodegeneration Using Bimolecular Fluorescence Complementation. , 506, pp.157–174.

Herrmann, H. et al., 2007. Intermediate filaments: from cell architecture to nanomechanics. *Nature Reviews Molecular Cell Biology*, 8(7), pp.562–573. Available at: http://www.nature.com/doifinder/10.1038/nrm2197.

Hol, E.M. et al., 2003. Neuronal expression of GFAP in patients with Alzheimer pathology and identification of novel GFAP splice forms. *Molecular Psychiatry*, 8(9), pp.786–796. Available at: http://www.nature.com/doifinder/10.1038/sj.mp.4001379.

Hol, E.M. & Pekny, M., 2015. Glial fibrillary acidic protein (GFAP) and the astrocyte intermediate filament system in diseases of the central nervous system. *Current Opinion in Cell Biology*, 32, pp.121–130. Available at: http://linkinghub.elsevier.com/retrieve/pii/S0955067415000137.

Inagaki, M. et al., 1994. Glial fibrillary acidic protein: dynamic property and regulation by phosphorylation. *Brain pathology (Zurich, Switzerland)*, 4(3), pp.239–43. Available at: http://www.ncbi.nlm.nih.gov/pubmed/7952265.

Inagaki, M. et al., 1990. Phosphorylation sites linked to glial filament disassembly in vitro locate in a non-??-helical head domain. *Journal of Biological Chemistry*, 265(8), pp.4722–4729.

Isaacs, A. et al., 1998. Determination of the gene structure of human GFAP and absence of coding region mutations associated with frontotemporal dementia with parkinsonism linked to chromosome 17. *Genomics*, 51(1), pp.152–154.

Jany, P.L., Hagemann, T.L. & Messing, A., 2013. GFAP expression as an indicator of disease severity in mouse models of Alexander disease. *ASN neuro*, 5(1), p.e00109. Available at: http://www.pubmedcentral.nih.gov/articlerender.fcgi?artid=3604736&tool=pmcentrez&rendertype=abstract [Accessed September 16, 2014].

Kato, H. et al., 1990. Immunocytochemical characterization of supporting cells in the enteric nervous system in Hirschsprung's disease. *Journal of pediatric surgery*,

25(5), pp.514–519.

Kodama, Y. & Hu, C.D., 2010. An improved bimolecular fluorescence complementation assay with a high signal-to-noise ratio. *BioTechniques*, 49(5), pp.793–803.

Ku, N.O. & Omary, M.B., 2006. A disease- and phosphorylation-related nonmechanical function for keratin 8. *Journal of Cell Biology*, 174(1), pp.115–125.

Kumanishi, T. et al., 1992. Human glial fibrillary acidic protein (GFAP): molecular cloning of the complete cDNA sequence and chromosomal localization (chromosome 17) of the GFAP gene. *Acta Neuropathologica*, 83, pp.569– 578.

McCall, M. a et al., 1996. Targeted deletion in astrocyte intermediate filament (Gfap) alters neuronal physiology. *Proceedings of the National Academy of Sciences of the United States of America*, 93(June 1996), pp.6361–6366.

Messing, a et al., 1998. Fatal encephalopathy with astrocyte inclusions in GFAP transgenic mice. *The American journal of pathology*, 152(2), pp.391–398.

Morell, M. et al., 2008. Study and selection of in vivo protein interactions by coupling bimolecular fluorescence complementation and flow cytometry. *Nature protocols*, 3(1), pp.22–33. Available at: http://www.ncbi.nlm.nih.gov/pubmed/18193018.

Nakagawa, C. et al., 2011. Improvement of a Venus-based bimolecular fluorescence complementation assay to visualize bFos-bJun interaction in living cells. *Bioscience, biotechnology, and biochemistry*, 75(7), pp.1399–401. Available at: http://www.ncbi.nlm.nih.gov/pubmed/21737916.

Nawashiro, H. et al., 1998. Mice lacking GFAP are hypersensitive to traumatic cerebrospinal injury. *Neuroreport*, 9(8), pp.1691–1696.

Nedergaard, M., Ransom, B. & Goldman, S.A., 2003. New roles for astrocytes: redefining the functional architecture of the brain. *Trends in neurosciences*, 26(10), pp.523–530.

Nielsen, A.L. et al., 2002. A new splice variant of glial fibrillary acidic protein, GFAP epsilon, interacts with the presenilin proteins. *Journal of Biological Chemistry*, 277(33), pp.29983–29991.

Nishizawa, K. et al., 1991. Specific localization of phosphointermediate filament protein in the constricted area of dividing cells. *Journal of Biological Chemistry*, 266(5), pp.3074–3079.

Nogales, E., 2001. STRUCTURAL INSIGHTS INTO MICROTUBULE FUNCTION. *Annual Reviews Biochem*, 69, pp.277–302.

Ohashi, K. et al., 2012. Visualization of cofilin-actin and Ras-Raf interactions by bimolecular fluorescence complementation assays using a new pair of split Venus fragments. *BioTechniques*, 52(1). Available at: http://www.biotechniques.com/article/000113777.

Outeiro, T.F. et al., 2008. Formation of toxic oligomeric alpha-synuclein species in living cells. *PloS one*, 3(4), p.e1867. Available at: http://www.pubmedcentral.nih.gov/articlerender.fcgi?artid=2270899&tool=pmcentrez&rendertype=abstract [Accessed July 20, 2014].

De Pablo, Y. et al., 2013. Intermediate filaments are important for astrocyte response to oxidative stress induced by oxygen-glucose deprivation and reperfusion. *Histochemistry and Cell Biology*, 140(1), pp.81–91.

Perea, G., Navarrete, M. & Araque, A., 2009. Tripartite synapses: astrocytes process and control synaptic information. *Trends in neurosciences*, 32(8), pp.421–431.

Perng, M. et al., 2008. Glial Fibrillary Acidic Protein Filaments Can Tolerate the Incorporation of Assembly-compromised GFAP- □ , but with Consequences for Filament Organization and ‗ B-Crystallin Association. , 19(October), pp.4521–4533.

Powell, E.M. & Geller, H.M., 1999. Dissection of astrocyte-mediated cues in neuronal guidance and process extension. *Glia*, 26(1), pp.73–83.

Prust, M. et al., 2011. GFAP mutations, age at onset, and clinical subtypes in Alexander disease. *Neurology*, 77(13), pp.1287–94. Available at: http://www.pubmedcentral.nih.gov/articlerender.fcgi?artid=3179649&tool=pmcentrez&rendertype=abstract.

Quinlan, R. a et al., 2007. GFAP and its role in Alexander disease. *Experimental cell research*, 313(10), pp.2077–87. Available at: http://www.pubmedcentral.nih.gov/articlerender.fcgi?artid=2702672&tool=pmcentrez&rendertype=abstract [Accessed September 1, 2014].

Reeves, S. a et al., 1989. Molecular cloning and primary structure of human glial fibrillary acidic protein. *Proceedings of the National Academy of Sciences of the United States of America*, 86(13), pp.5178–5182.

Repici, M. et al., 2013. Parkinson's disease-associated mutations in DJ-1 modulate its dimerization in living cells. *Journal of molecular medicine (Berlin, Germany)*, 91(5), pp.599–611. Available at: http://www.pubmedcentral.nih.gov/articlerender.fcgi?artid=3644405&tool=pmcentrez&rendertype=abstract.

Riol, H. et al., 1997. Detection of the peripheral nervous system (PNS)-type glial fibrillary acidic protein (GFAP) and its mRNA in human lymphocytes. *Journal of neuroscience research*, 48(1), pp.53–62.

Roelofs, R.F. et al., 2005. Adult human subventricular, subgranular, and subpial zones contain astrocytes with a specialized intermediate filament cytoskeleton. *Glia*, 52(4), pp.289–300.

Rueger, D.C. et al., 1979. Formation of 100Å filaments from purified glial fibrillary acidic protein in vitro. *Journal of Molecular Biology*, 135, pp.53–68.

Russo, L.S.J., Aron, A. & Anderson, P.J., 1976. Alexander's disease: a report and reappraisal. *Neurology*, 26(7), pp.607–614.

Sajjad, M.U. et al., 2014. DJ-1 modulates aggregation and pathogenesis in models of Huntington's disease. *Human Molecular Genetics*, 23(3), pp.755–766. Available at: http://eutils.ncbi.nlm.nih.gov/entrez/eutils/elink.fcgi?dbfrom=pubmed&id=24070869&retmode=ref&cmd=prlinks\npapers2://publication/doi/10.1093/hmg/ddt466.

Saka, Y., Hagemann, A.I. & Smith, J.C., 2008. Visualizing protein interactions by bimolecular fluorescence complementation in Xenopus. *Methods*, 45, pp.192–195.

Sawaishi, Y., 2009. Review of Alexander disease: beyond the classical concept of leukodystrophy. *Brain & development*, 31(7), pp.493–8. Available at: http://www.ncbi.nlm.nih.gov/pubmed/19386454 [Accessed August 22, 2014].

Seri, B. et al., 2001. Astrocytes give rise to new neurons in the adult mammalian hippocampus. *The Journal of Neuroscience*, 21(18), pp.7153–7160.

Sheridan, D.L. et al., 2002. A new way to rapidly create functional, fluorescent fusion proteins: random insertion of GFP with an in vitro transposition reaction. *BMC Neuroscience*, 3(1), p.7. Available at: http://www.biomedcentral.com/1471-2202/3/7/abstract\nhttp://www.biomedcentral.com/1471-2202/3/7\nhttp://www.biomedcentral.com/content/pdf/1471-2202-3-7.pdf.

Shyu, J.Y. et al., 2006. Identification of new fluorescent protein fragments for bimolecular fluorescence complementation analysis under physiological conditions. *BioTechniques*, 40, pp.61–66.

Shyu, Y.J. et al., 2006. Identification of new fluorescent protein fragments for bimolecular fluorescence complementation analysis under physiological conditions. *BioTechniques*, 40(1), pp.61–66.

Sofroniew, M. V. & Vinters, H. V., 2010. Astrocytes: biology and pathology. *Acta Neuropathologica*, 119(1), pp.7–35. Available at: http://link.springer.com/10.1007/s00401-009-0619-8.

Szeverenyi, I. et al., 2008. The Human Intermediate Filament Database: comprehensive information on a gene family involved in many human diseases.

Human Mutation, 29(3), pp.351–360. Available at: http://doi.wiley.com/10.1002/humu.20652.

Tang, G., Xu, Z. & Goldman, J.E., 2006. Synergistic Effects of the SAPK/JNK and the Proteasome Pathway on Glial Fibrillary Acidic Protein (GFAP) Accumulation in Alexander Disease. *Journal of Biological Chemistry*, 281(50), pp.38634–38643. Available at: http://www.jbc.org/cgi/doi/10.1074/jbc.M604942200.

Triolo, D. et al., 2006. Loss of glial fibrillary acidic protein (GFAP) impairs Schwann cell proliferation and delays nerve regeneration after damage. *Journal of cell science*, 119(Pt 19), pp.3981–3993.

Wilhelmsson, U. et al., 2004. Absence of glial fibrillary acidic protein and vimentin prevents hypertrophy of astrocytic processes and improves post-traumatic regeneration. *The Journal of neuroscience : the official journal of the Society for Neuroscience*, 24(21), pp.5016–21. Available at: http://www.ncbi.nlm.nih.gov/pubmed/15163694 [Accessed September 4, 2014].

Yoshida, T. et al., 2011. Nationwide survey of Alexander disease in Japan and proposed new guidelines for diagnosis. *J Neurol*, 258(11), pp.1998–2008. Available at: http://www.ncbi.nlm.nih.gov/pubmed/21533827.

Zelenika, D. et al., 1995. A novel glial fibrillary acidic protein mRNA lacking exon 1. *Molecular Brain Research*, 30(2), pp.251–258. Available at: http://www.sciencedirect.com/science/article/pii/0169328X9500010P.